The role of behavioral relevance for sensory processing in the mouse visual system

Dissertation

zur Erlangung des Grades eines
Doktors der Naturwissenschaften

der Mathematisch-Naturwissenschaftlichen Fakultät
und
der Medizinischen Fakultät
der Eberhardt-Karls-Universität Tübingen

vorgelegt
von

Alexandra Wal
aus Heydebreck, Polen

Tübingen, Februar 2018

Tag der mündlichen Prüfung:	06.06.2018
Dekan der Math.-Nat. Fakultät:	Prof. Dr. W. Rosenstiel
Dekan der Medizinischen Fakultät:	Prof. Dr. I. B. Autenrieth
1. Berichterstatter:	Dr. Steffen Katzner
2. Berichterstatter:	Prof. Dr. Ziad Hafed
Prüfungskommission:	Dr. Steffen Katzner
	Prof. Dr. Ziad Hafed
	Prof. Dr. Joachim Ostwald
	Dr. Hendrikje Nienborg

Erklärung / Declaration:

Ich erkläre, dass ich die zur Promotion eingereichte Arbeit mit dem Titel:

„The role of behavioral relevance for sensory processing in the mouse visual system"

selbständig verfasst, nur die angegebenen Quellen und Hilfsmittel benutzt und wörtlich oder inhaltlich übernommene Stellen als solche gekennzeichnet habe. Ich versichere an Eides statt, dass diese Angaben wahr sind und dass ich nichts verschwiegen habe. Mir ist bekannt, dass die falsche Abgabe einer Versicherung an Eides statt mit Freiheitsstrafe bis zu drei Jahren oder mit Geldstrafe bestraft wird.

*I hereby declare that I have produced the work entitled "*The role of behavioral relevance for sensory processing in the mouse visual system*", submitted for the award of a doctorate, on my own (without external help), have used only the sources and aids indicated and have marked passages included from other works, whether verbatim or in content, as such. I swear upon oath that these statements are true and that I have not concealed anything. I am aware that making a false declaration under oath is punishable by a term of imprisonment of up to three years or by a fine.*

Tübingen, den ....

Datum / Date Unterschrift /Signature

Table of Contents

List of Figures

1 Summary

Sensory processing does not only reflect the physical properties of a given stimulus, but can be affected by the behavioral relevance of visual information. These changes in sensory processing can enhance responses to stimuli, which are relevant for behavior, and suppress activity to irrelevant noise. Task-related modulations in sensory processing have been fundamentally investigated in monkey studies, though, more sophisticated experimental methods have pushed towards investigating neural functions of perception in the mouse. An increasing number of studies has documented state-dependent changes in responses of neurons in visual cortex, but how sensory processes change when stimuli become behaviorally relevant is not well understood.

In this study I was interested in how the behavioral context of a visual stimulus changes neuronal processing in the early visual system of the mouse. To address this question, I designed a visual foraging task, in which mice learned to discriminate between two stimuli, which provided identical sensory stimulation, but differed in reward contingencies. After mice learned to perform the task, I obtained electrophysiological recordings from the primary visual cortex (V1) to test if behavioral relevance of the stimulus changes firing rates. In a passive viewing condition, I measured sensory responses to the two stimuli outside the context of the task. These measurements were used to exclude from further analyses all neurons that showed any difference in their sensory response to the two stimuli. I found that of the recorded V1 population which did not distinguish between the two stimuli during passive viewing, 25% of neurons signaled stimulus identity during task engagement. To further investigate if these changes arise in cortex or might be inherited from their main input area, the lateral geniculate nucleus (dLGN), I recorded from the dLGN during the same task. As in V1, neurons in dLGN showed changes in firing rates when stimuli became behaviorally relevant. However, the subset of neurons affected was low (10%). Knowing that stimulus context can shape response properties in mouse V1, I further investigated the role of intracortical inhibition. Narrow-spiking, putative inhibitory, and broad-spiking, putative excitatory, neurons exhibited similar strengths of changes in firing rates when stimuli became behaviorally relevant during task engagement. These findings show that the visual foraging task can be used to manipulate behavioral relevance while keeping the sensory input for single neurons constant. These manipulations can affect sensory processing within the mouse early visual system, including inhibition by putative inhibitory interneurons.

2 Introduction

2.1 Visual perception is more than a readout of physical information

Any sensory experience, such as the perception of a visual scene, relies on the coordinated activity of neurons in the cerebral cortex. Traditionally, sensory areas have been thought to function as simple feature detectors and to construct a direct representation of the visual world. In a feedforward pathway visual information first exits the retina through the optic nerve, whose fibers partly cross in the optic chiasm to build the contralateral and ipsilateral optic tracts. The ganglion cell axons in the optic tract reach several subcortical structures, with the dorsal lateral geniculate nucleus (dLGN) of the thalamus as a major target (Hubel and Wiesel, 1977). From the dLGN, which was characterized for a long time as a relay station, visual information enters the primary visual cortex (V1) which extracts low complexity features of a stimulus such as contrast or specific orientations (Hubel and Wiesel, 1959). Different classes of neurons organized in layers and columns within this pathway encode the varieties of visual information that we see. The processing of different categories of visual information continues in cortical pathways through the extrastriate cortex which encodes more complex features such as contours, textures and combination of orientations in visual area V2 (e.g. Anzai et al., 2007; Freeman et al., 2013; Willmore et al., 2010), curvatures in visual area V4 (e.g. Pasupathy and Connor, 1999) and faces in the inferior temporal cortex (IT) (e.g. Desimone et al., 1984; Felleman and Van Essen, 1991; Tanaka, 1996). Somewhere beyond the extrastriate cortex, cognitive processes in higher brain areas like the prefrontal cortex allow us to interpret and understand the sensory information in the context of our current behavioral state (Miller and Cohen, 2001).

In contrast to a classical feedforward pathway, decades of research have documented that the functional properties of neurons in the cortex are not fixed, but can be influenced by the current behavioral context. In our daily environment each time we open our eyes we are confronted with an immense amount of sensory information. At the same time, we seem to have an effortless understanding of our visual world. Due to the limited processing capacity of the brain, we need a selective process that filters relevant information out of irrelevant noise. A fundamental property of visual cortex is to enhance the representation of those stimuli which are relevant for behavior. In this case, bottom-up processes are accompanied by top-down processes which can shape sensory processing. As

one example, visual attention refers to a selective process that helps guide us through the world by emphasizing behaviorally relevant stimuli and ignoring distractors (for review, see Gilbert and Li, 2013; Maunsell, 2015). In this context, an animal's association between a sensory stimulus and its behavioral relevance can change stimulus representations in sensory cortical areas. In general, visual perception is not only a passive readout of sensory information, but is also shaped by the animal's learning, memory, expectation or attention.

2.2 Attention modulates sensory processing in the early visual system

The neuronal mechanisms that underlie attention have long been the subject of studies (e.g., Moran and Desimone, 1985). Attention has been shown to influence neural processing of sensory stimuli and can be studied under constant sensory and motor conditions (for reviews see: Baluch and Itti, 2011; Carrasco, 2011; Gilbert and Li, 2013; Maunsell, 2015; Noudoost et al., 2010). This allows the isolation of signatures of a behavioral component and its correlation with changes in neuronal activity. In experiments, the influence of attention has been tested by training subjects in a process called covert attention, in which they attend to an area in the periphery, without directing gaze towards it. With electrophysiological recordings, shifts of attention towards or away from a visual stimulus within a neuron's receptive field could show changes in responses to that stimulus. In monkeys, electrophysiological recordings in visual area V4 showed that neurons responded more strongly when the animal paid attention to the stimulus within the receptive field (e.g., McAdams and Maunsell, 1999; Moran and Desimone, 1985; Motter, 1994). Rapid changes of firing rates related to attention have been demonstrated in a number of cortical areas, including V2 (e.g. Buffalo et al., 2010; Luck et al., 1997), the medial temporal (MT) area (e.g. Busse et al., 2008; Treue and Martínez Trujillo, 1999), the inferior temporal (IT) area (e.g. Chelazzi et al., 1998) and the lateral intraparietal area (LIP) (e.g. Bisley and Goldberg, 2003). These results demonstrated that covert attention modulates neuronal activity and therefore enhances the representation of the stimulus for the purpose of selection throughout the visual cortex. Additionally, attentional modulation has been observed in the first cortical stage of visual processing, area V1, and corrected the view of this area being purely sensory (Motter, 1993; Roelfsema et al., 1998). Commonly, along the cortical areas, most neurons responded more strongly when attention was directed towards the stimulus in the receptive field. The average response enhancement, however, differed along cortical areas, with effect size increasing from lower to higher visual areas (for summary see: Maunsell and Cook,

2002; Noudoost et al., 2010). In addition, the fraction of affected neurons increases along the visual processing hierarchy (Buffalo et al., 2010). Furthermore, effects of attention reach back to one of the first visual processing stages, namely the dorsal lateral geniculate nucleus (dLGN) (McAlonan et al., 2008; O'Connor et al., 2002). These studies revealed that attention modulates visual signals before they even enter the cortex. Together, these studies of how attentional shifts can influence sensory processing have built powerful examples linking cortical activity with the behavioral relevance of the visual stimulus.

2.3 The mouse as a model system for vision neuroscience

Over the last 15 years, the mouse has gained popularity as a model system for visual neuroscience (Hübener, 2003). Humans use vision as their primary sense to guide behavior, which is why investigating the neural basis of visual perception is a fundamental goal in neuroscience. Until now, vision research has relied mainly on animal models such as cats or non-human primates, whose visual systems are elaborate and express key response properties similar to those of humans. Mice, in contrast, are believed to rely mainly on tactile information and olfactory cues because they are predominantly nocturnal (Hut et al., 2011) and have small eyes (Remtulla, 1985) with a low photoreceptor density which makes them look at the world with very low resolution (Prusky and Douglas, 2004). Given the advantages of other animal models, why should someone investigate the neural basis of vision in the mouse? First, mice, and also their brains, are small and the visual cortex lies on the surface of the brain which allows easy access and visualization of the whole visual system simultaneously (e.g., Wekselblatt et al., 2016). Second, a strong argument to use the mouse model is the availability of genetic engineering methods which provide abundant opportunities to investigate neural circuits (for review: Deisseroth, 2015). To investigate brain functions, scientists have used the techniques of recording and manipulating neural activity during different conditions. Brain activity has been manipulated electrically (e.g., Moore and Fallah, 2001), chemically (e.g., Newsome and Pare, 1988), with structural disruptions (e.g., Kawai et al., 2015), or optogenetically (e.g. Zhang et al., 2007). Of all these methods, optogenetics is the newest and strongest tool to control neural activity on millisecond timescales (see Deisseroth, 2015). Furthermore, in the monkey model, while distinct wave shapes allow differentiation among broad cell categories, like putative inhibitory or excitatory cells (Chen et al., 2008; Mitchell et al., 2007), it is not currently possible to target defined cell classes for more detailed investigations. The widespread availability of transgenic mouse lines enables targeting of specific cell types and brain areas with their downstream and

upstream targets with high temporal and spatial precision and therefore allows a more elaborate method of investigating brain circuit functions. Because the availability of these powerful methods provides the opportunity to resolve long-lasting questions of visual processing, interest in this animal model has grown in the recent years. Remarkably, recent studies have demonstrated that the mouse visual system is more elaborated than previously thought. Therefore, the mouse model offers sophisticated possibilities to study basic functions of visual processing.

2.4 The mouse visual system

Mouse vision has low acuity and might not be used as their primary sense, though it shares some basic similarities in structure and function to the visual systems of higher mammals (Gao et al., 2010; Huberman and Niell, 2011; Niell, 2014; Wang et al., 2011) or humans (for summary see Katzner and Weigelt, 2013). The mouse retina consists of mainly rods (97%), which are well adapted for night vision, and the lack of a fovea makes them see as unclear as humans' peripheral vision (Jeon et al., 1998; Prusky and Douglas, 2004). This leads to a behavioral acuity nearly two orders of magnitude lower than in cats or monkeys (Prusky et al., 2000). Nevertheless, the mouse visual pathway shows strong similarities in structures and steps in the processing hierarchy of visual information compared to higher mammals. The dLGN is positioned between the retina and the primary visual cortex to process and relay visual information (for review see: Seabrook et al., 2017)(**Figure 1**). It contains neurons with classical receptive field properties (Grubb, 2003), but also neurons which encode more complex properties, including direction and orientation selectivity or center-surround information (Marshel et al., 2012; Piscopo et al., 2013; Scholl et al., 2013; Zhao et al., 2013). The main target of dLGN projections is the primary visual cortex. As in primates, the visual cortex reveals a typical 6-layered structure (Olivas et al., 2012), retinotopic organization (Drager, 1975; Schuett et al., 2002; Wang and Burkhalter, 2007) and a variety of excitatory and inhibitory neuronal subtypes (Markram et al., 2004). Visual information enters the cortex mainly in layer 4 (Lien and Scanziani, 2013), where vertical and horizontal processing streams seem crucial for coordination of responses to sensory stimuli (e.g., Bortone et al., 2014; Cossell et al., 2015; Olsen et al., 2012). Beside this, neurons in V1 show typical response properties like selectivity for stimulus parameters such as orientation and spatial frequency which compare with key response properties in higher mammals (Van Den Bergh et al., 2010; Bonin et al., 2011; Drager, 1975; Métin et al., 1988; Niell and Stryker, 2008). The degree of orientation selectivity is similar to that of cats or primates

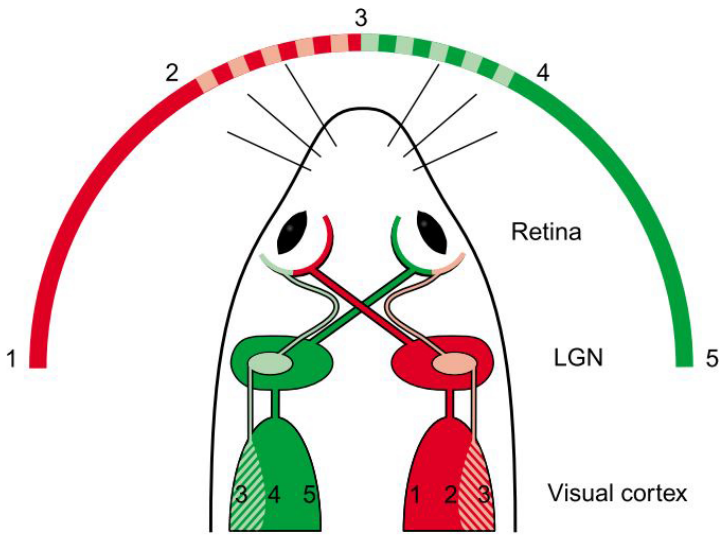

Figure 1: Schematic of the mouse visual system. Left and right visual hemifields and their representations in the brain are colored in red and green. The majority of retinal ganglion cells cross over to the other hemisphere, while fibers from the most temporal region project to the ipsilateral hemisphere (light green and red). © 2003 Elsevier Ltd. Adapted with permission from (Hübener, 2003).

(Niell and Stryker, 2008), though mouse V1 lacks a higher organization such as orientation columns (Ohki and Reid, 2007). In addition to primary visual cortex, the mouse visual system consists of around nine separated, retinotopically organized areas (Wang and Burkhalter, 2007) (**Figure 2**). The principal targets of V1 are the lateromedial (LM) and the anterolateral (AL) areas, which in turn show stronger connections to temporal (P, POR, LI) and parietal (RL, A, AM) areas, respectively (Wang et al., 2011). Beside distinct connectivity streams, two-photon calcium imaging studies revealed functional specializations among these visual areas. Neurons in posterior parietal areas (AL, RL, AM) show strong direction selectivity and prefer high temporal and low spatial frequencies, whereas neurons in temporal areas (LI, PM) prefer low temporal and high spatial frequencies (Andermann et al., 2011; Marshel et al., 2011; Roth et al., 2012). This specific transmission of visual information to downstream targets arises from functionally target-specific cortico-cortical projections and may be a general feature of cortico-cortical communication (Glickfeld et al., 2013a). The specialization towards the processing of motion or structural details might suggest similar hierarchical pathways for sensory processing as is the case in the ventral and dorsal stream in primates (Felleman and Van Essen, 1991).

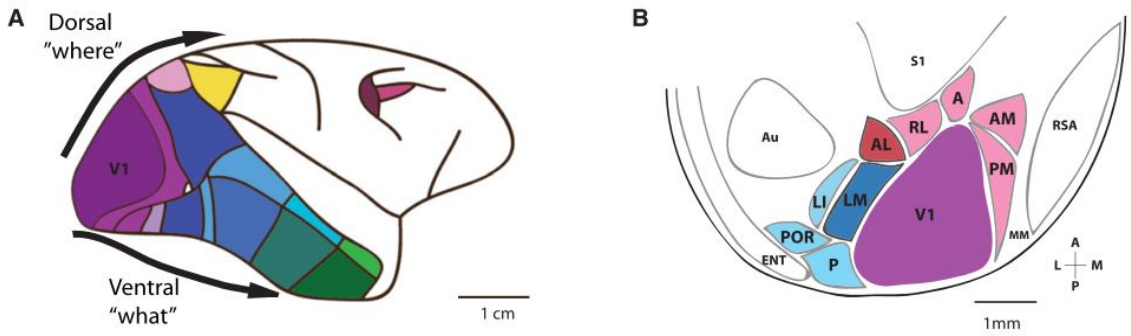

Figure 2: Striate and extrastriate areas in the primate (left) and mouse (right). A=anterior area, AL= anterolateral area, AM, anteromedial area, Au=auditory cortex, ENT=entorhinal cortex, LI=laterointermediate area, LM=lateromedial area, MM=mediomedial area, P=posterior area, PM=posteromedial area, POR=postrhinal area, RL=rostrolateral area, RSA=retrosplenial agranular cortex, S1=primary somatosensory area, V1=primary visual area © 2011 Elsevier Inc. Adapted with permission from (Niell, 2011).

2.5 Mouse vision depends on context

Recent work in the mouse has revealed signatures of behavioral correlates in sensory processing of the early visual system. For instance, behavioral state in awake mice influences single neuron activity in V1 and dLGN (Erisken et al., 2014; Niell and Stryker, 2010). When head-fixed mice, positioned on a spherical treadmill, transitioned from being stationary to running, visually-evoked as well as spontaneous neuronal activity increased while maintaining orientation selectivity (**Figure 3**). This increase is further accompanied by a change in spatial integration, indicating a change in tuning selectivity (Ayaz et al., 2013; Erisken et al., 2014), and changes in subthreshold properties of neurons with a shift in resting membrane potential (Polack et al., 2013). Furthermore, sensorimotor mismatch signals have been described in V1. In a visual-flow feedback paradigm, the visual flow of a stimulus was coupled to the running speed of the mouse. Perturbations of the coupling (feedback mismatch) resulted in strong responses of V1 neurons, suggesting that cortical sensory processing involves predictions and therefore goes beyond simple feedforward processing (Keller et al., 2012).

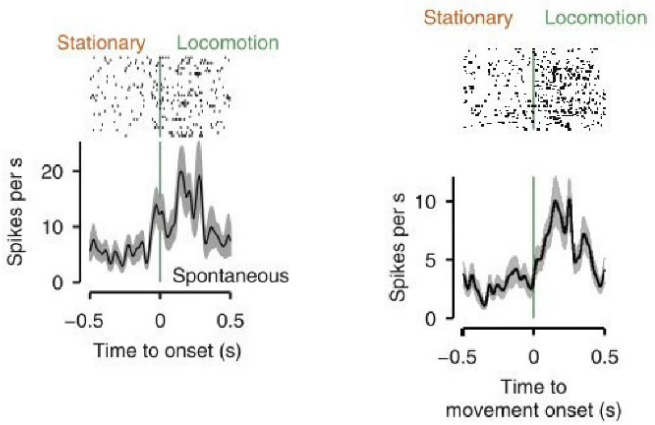

Figure 3: Locomotion enhances firing rates of neurons in mouse LGN and V1 (left and right, respectively). Spike rasters (top) and spike density function (bottom) of an example dLGN (left) and V1 (right) neuron during spontaneous activity aligned to locomotion onset. © 2014 Elsevier Ltd. Adapted with permission from (Erisken et al., 2014).

In addition, V1 activity has been tested in the context of more complex behavioral paradigms and visual discrimination. In the work of Poort et al. (2015), learning has been shown to increase stimulus discriminability on the population level. Mice were trained in a virtual reality visual discrimination task, where they learned to earn rewards by stopping running in a virtual corridor when one of two different gratings appeared. During learning over a few days, the population level neuronal discriminability as well as the fraction of task-selective neurons increased. These enhancements of stimulus representation in V1 diminished when mice were not active in the visual discrimination task. These fast improvements in neural discrimination of sensory signals when stimuli become behaviorally relevant suggest that task dependent changes influence sensory processing in mouse V1, presumably through top-down modulation. Changes in neuronal discriminability have been shown as well in the context of a classical conditioning paradigm (Jurjut et al., 2017). This study revealed learning-related improvements in V1 discriminability, before discrimination was evident in the animal's behavior. Besides, orientation discrimination under classical conditioning required activity of V1 neurons, as the animals showed impaired task performance when silencing V1 neurons with optogenetics. The dependence on V1 activity during a visually guided detection task has been demonstrated as well by Glickfeld et al. (2013b) and points toward a key role of V1 in performing visual tasks and discrimination learning. Furthermore, reward prediction is able to alter V1 activity even in the absence of visual stimulation (Shuler and Bear, 2006). Summarizing these studies demonstrate that early visual areas of the mouse are not purely sensory, but can be influenced by the behavioral state (active vs. passive), long-term network plasticity with learning, or task engagement.

2.6 Feedback projections can modulate sensory processing

Anatomical studies revealed that cortical processing is not strictly hierarchical, but that feedforward connections from one area to the next are accompanied by parallel feedback connections in the reverse direction (Callaway, 2004; Lamme et al., 1998). Linking these anatomical circuits to function revealed that feedforward connections are rather driving, with a strong synaptic power, in comparison to feedback projections which are rather modulatory (Callaway, 1998; Sherman and Guillery, 1998). Feedback projection can comprise a large proportion of synaptic connections in one area; e.g. in the LGN up to 60% of synapses arise from feedback projections, half of which come from the primary visual cortex and originate mainly from layer 6 (L6) (Sherman and Guillery, 2002). Blocking feedback activity from V1 L6 neurons results in only a small reduction of firing rate in the dLGN, but a significant decrease in surround suppression when stimulus size extended beyond the classical receptive field size (Sillito and Jones, 2002). As another example, in the monkey electrical stimulation of the frontal eye field (FEF) enhanced V4 neuron responses in the retinotopically corresponding location and suppressed responses at other locations (Moore and Armstrong, 2003), simulating the center-surround profile of attentional modulation (e.g., McAdams and Maunsell, 1999).

Several brain areas in the mouse directly innervate early sensory areas through long-range projections and are potential candidates to carry context dependent information. With precise optogenetic tools, the role of these feedback projections from higher brain areas has been tested in the context of task dependent modulations in the mouse. One example is the cingulate (Cg) area, which is known to be implicated in effort-based decision making (Shenhav et al., 2016). In anesthetized mice, optogenetic activation of the cingulate area increased V1 responses to stimuli at the preferred orientation, which resulted in an approximately multiplicative scaling of the tuning curve, similar to the effects of top-down attention (Zhang et al., 2014). Furthermore, in a separate behavioral experiment, Cg activation also improved behavioral performance in a visual discrimination task. Further anatomical characterization of the long-range projections from the cingulate area have revealed distinct subnetworks with subpopulations projecting to the visual cortex and the superior colliculus (Zhang et al., 2016) (**Figure 4**). These anatomical characterizations provide insight into separate physiological functions of Cg projections which might be separately implemented in the control of visual perception and action subnetworks. A similar approach demonstrated that cholinergic long-range projections from the basal forebrain improved task performance. Optogenetic manipulations of basal

forebrain cholinergic neurons caused enhanced cortical processing on a small timescale and could therefore play a role in activating the cortex and improving sensory processing in visual tasks (Pinto et al., 2013).

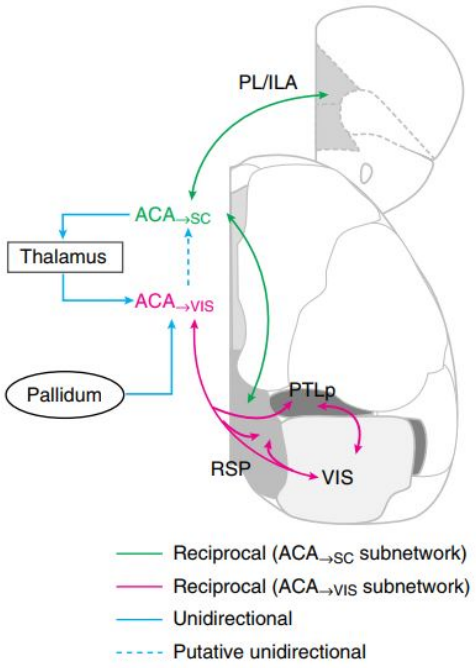

Figure 4: Schematic diagram of visual circuits in the mouse. Shown are major connections from ACA neurons. ACA=Anterior cingulate area; ILA=Infralimbic area; PL=Prelimbic area; SC=Superior colliculus; VIS=Visual areas; PTLp=Posterior parietal association areas; RSP=Retrosplenial area. © 2016, Springer Nature. Adapted with permission from (Zhang et al., 2016).

In addition, the prefrontal cortex (PFC) is known to exhibit diverse behavioral correlates (e.g., Kvitsiani et al., 2013; Rodgers and DeWeese, 2014; Wallis and Kennerley, 2010) and has been tested in its interactions with sensory areas in sensory selection (Wimmer et al., 2015). In a learned divided attention task, mice were not able to select the appropriate modality when PFC function was temporarily perturbed. More precisely, appropriate behavioral performance relied on the interaction between the PFC and the thalamus, not the sensory cortex and introduced a new subcortical model of sensory selection. In general, feedback connections are likely candidates to contribute to rapid modulatory effects throughout the cortex and the subcortex and optogenetic methods help to gain better insight into context dependent mechanisms.

2.7 Interneurons are likely targets for task dependent modulations

The cortex contains multiple cell types which build a complex network of excitatory and inhibitory neurons. About 80% of cortical neurons are excitatory pyramidal neurons, and the remaining ones are mostly inhibitory GABAergic interneurons with very diverse characteristics (Markram et al., 2004). In contrast to excitatory neurons, inhibitory interneurons usually arborize their axons within a cortical column with lateral extensions. Because they mostly do not project to other brain areas, they are also called 'local circuit neurons'. Inhibition plays an important role in neural processing of sensory information for example in gain control and stimulus selectivity of cortical neurons (Katzner et al., 2011), but also in the maintenance of oscillatory cortical activity (Isaacson and Scanziani, 2011). An abnormal inhibitory circuit has been implicated in many neurological disorders such as epilepsy and schizophrenia (Moult, 2009). Transgenic mouse lines have allowed the elaboration of the function of certain types of neurons and helped to understand the important aspects of connectivity and function among interneurons. Most interneurons in the rodent cortex fall into three nonoverlapping categories, namely neurons with the calcium-binding protein parvalbumin (PV+), neurons with the neuropeptide somatostatin (SOM+), and vasoactive intestinal polypeptide (VIP+) containing neurons (Rudy et al., 2011). The activity among these three subgroups is highly coordinated (Karnani et al., 2016), while their roles in cortical inhibition in turn are distinct. SOM+ neurons provide a weaker inhibition to excitatory cells by innervating their dendrites, but also inhibit other inhibitory VIP+ and PV+ neurons. A strong inhibitory drive is given by PV+ neurons which directly synapse onto the soma of excitatory cells, but at the same time inhibit themselves and provide a positive feedback mechanism. VIP+ neurons inhibit SOM+ neurons and therefore have a disinhibitory function in the cortex (Pfeffer et al., 2013).

Recent studies have shed light on local circuit mechanisms that could account for context dependent modulations in sensory processing. All three subtypes of interneurons receive direct long-range feedback innervation from the cingulate (Cg) area in the mouse (Zhang et al., 2014). Focal activation of Cg axons modulated V1 responses in a center-surround manner. Testing the role of each interneuron subtype in this modulation revealed a contribution of SOM+ neurons in surround suppression, whereas VIP+ neurons were crucial for center facilitation. VIP+ neurons have also been shown to increase their activity during locomotion, and ablation of VIP+ neuron activity in turn reduced the effect of locomotion on sensory processing in V1 (Fu et al., 2014). This work also showed the direct

innervation of VIP+ neurons by cholinergic input from the basal forebrain, which has been shown to induce changes in cortical activity similar to those induced by locomotion (Pinto et al., 2013). In spatial integration, activating SOM+ neurons resulted in an increase of the suppression index in surround suppression, whereas PV+ neuron activation decreased the strength of the input and mimicked effects of spatial integration at low contrasts (Nienborg et al., 2013; Vaiceliunaite et al., 2013). Additionally, in primates, top-down attention enhanced the firing rate of putative inhibitory interneurons in area V1 and V4 (Chen et al., 2008; Mitchell et al., 2007). In the somatosensory area, PV+ neurons fired at lower rates in hit trials in comparison to miss trials suggesting that they allow better sensory transformation of whisker stimuli (Sachidhanandam et al., 2016). PV+ neuron activation in visual cortex showed improved perceptual discrimination in a behavioral experiment (Lee et al., 2012). In a different set of experiments, activation of PV+ neurons in the auditory cortex enhanced feedforward functional connectivity, thereby improving the bottom-up sensory drive (Hamilton et al., 2013).

Interneurons are critical regulators for balanced cortical activity and seem to play an important role in the functionality of selective perception during behavior, but the exact mechanisms of how interneurons enhance the processing of behaviorally relevant stimuli in visual tasks are not well understood.

2.8 Linking neuronal activity with visually guided behavior

The mouse model shows promise for linking neural circuit function to visual perception and behavior. It is possible to perform psychophysics with mice, which ranges from reflexive behaviors to complex visual discrimination tasks. In head-fixation paradigms the visual input can be controlled and recordings from the brain can be performed while the animal is behaving. Many attempts to design behavioral tasks manipulate the relevance of a stimulus by coupling a reward or punishment with one stimulus, but not another, which reinforces the mouse to show aversive or attracted behavior. The simplest task design to test perception involves a go/no-go task. In this case, the mouse reports the presence of a stimulus attribute by performing or withholding a single action like pressing or releasing a bar, licking a spout or stopping/starting running on a treadmill (Andermann et al., 2010; Khastkhodaei et al., 2016; Lee et al., 2012; Poort et al., 2015) (**Figure 5**). This kind of task is easy to learn for mice, but because there is no active trial initiation, phases in which mice are not motivated are difficult to determine and results can therefore be contaminated. A more sophisticated way to investigate perception is a two-alternative forced-choice task, in which animals can report a

stimulus attribute with two response alternatives, for example by initiating a task in a central port through a nose poke and then moving to the right or left to report a decision (Busse et al., 2011; Jaramillo and Zador, 2011; Raposo et al., 2014; Znamenskiy and Zador, 2013) (**Figure 5**C). A further refinement of this task is the two-alternative forced choice task, in which two stimuli are presented at the same time and the animal needs to choose the stimulus with the right attribute (Burgess et al., 2017; Marbach and Zador, 2016; Sanders and Kepecs, 2012). In comparison to the simple go/no-go task this approach is more resistant to falsely interpreted trials where the animal doesn't want to respond, because a decision needs to be reported on every trial.

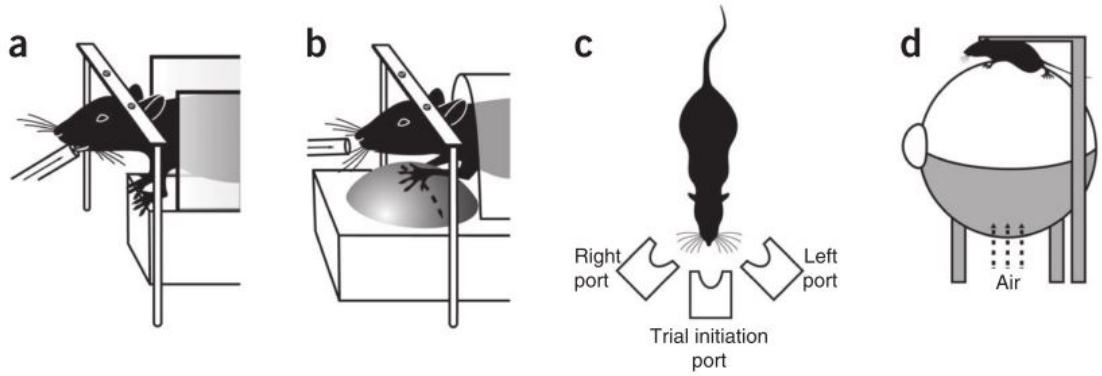

Figure 5: Techniques for rodent psychophysics. **(a)** A custom apparatus keeps the head still during stimulus presentation. Animals lick a spout to report detection of a stimulus. **(b)** Animals report decisions by moving a trackball to the left or right, allowing a continuous monitoring of their developing decisions. **(c)** A three-port apparatus wherein animals freely move first to a center port to initiate stimulus presentation, and the to the left or right reward port where decisions about the stimuli are reported. **(d)** A treadmill set-up in which animals are head-fixed, but able to move. Adapted from (Carandini and Churchland, 2013).

Learning times of behavioral paradigms range from a few days (Poort et al., 2015) to several weeks (Glickfeld et al., 2013b; Histed et al., 2012), but usually not longer than two months. All described task designs are constructed such that animals can perform hundreds of trials which is desirable for a robust characterization of the neuronal system. Recording from a large subset of neurons while animals are engaged in a behavioral task allows linking cellular and network mechanisms with visually guided behavior and perception. However, the development of precise psychophysical tasks in mice, as being performed in primate studies, is just emerging.

2.9 Can the mouse model help us to understand how vision works?

One hallmark of neuroscience research is to understand how brain functions guide behavior. This research has been traditionally performed in monkeys, where powerful examples have linked neuronal activity during attention or decision-making to behavior (see e.g. reviews: Carrasco, 2011; Gold and Shadlen, 2007; Nienborg et al., 2012). However, studies in the monkey model have been limited in their ability to dissect circuit functions which lead to behavioral outputs. The mouse provides the opportunity to find behavioral signatures in particular cell types and distinct circuit mechanisms. The fundamental properties of the primate visual system are present in the mouse and several psychophysical methods have been developed to test context-dependent neural activity. There is hope to gain better insight into how neural activity is linked to behavior and first attempts suggest that attentional modulation in primates and state-dependent cortical processing in rodents might share common mechanisms (Maimon, 2011). Nevertheless, it is important to point out that differences in the visual system of the mouse compared to primates and humans are numerous and not all findings within the mouse model may translate to higher mammalian species. Psychophysical methods for rodents are being developed, but presumably cannot reach the high standards of experimental control achieved in primate behavioral tasks. However, anatomical and functional studies in the mouse have enriched the field of vision neuroscience in many ways. In the future, the mouse model will help us to uncover some key aspects of how the brain works and will serve as a promising model whose insights into brain function can be translated to other species.

2.10 Does the behavioral relevance of a stimulus change visual processing in the mouse visual system?

Although the number of studies investigating how behavioral state can influence sensory processing in the mouse visual system is steadily increasing, it remains unclear how stimulus context can rapidly change neuronal representation in the mouse early visual system.

To address this question, I investigated how the behavioral context of a stimulus changes neuronal processing in the early visual system of the mouse. I designed a visual foraging task, in which mice learned to discriminate between two stimuli, which are the same in sensory drive but differ in reward contingencies. After mice learned to perform the task, I obtained, during task engagement,

electrophysiological recordings from area V1 to test if behavioral context changes firing rates. Of the recorded V1 population that did not discriminate between the two stimuli during passive viewing, I found that a substantial fraction (25%) signaled stimulus identity during task engagement. To assess whether these changes in stimulus representation arise in cortex or if they could be inherited from their main input area, the dLGN, I performed recordings from the dLGN during the same task conditions. Task dependent changes in firing rates were present in the dLGN, however, the proportion (10%) of affected neurons in comparison to V1 was small. Because interneurons are likely candidates to maintain context dependent modulations in the cortex, I further tested the role of intracortical inhibition in context dependent modulation. I recorded from identified PV+ cells and used them to validate the separation between narrow and broad spiking neurons by wave shape. Comparing both cell groups showed that narrow-spiking, putative inhibitory neurons showed similar discriminability in comparison to broad-spiking, putative excitatory neurons. These data demonstrate that the behavioral relevance of a given stimulus can shape neuronal responses before they enter the cortex. Furthermore, the results of this work indicate that inhibitory neurons exert similar strengths of context dependent modulation in the cortex, as they show similar changes in firing rates when stimuli became behaviorally relevant.

3 Results

3.1 Experimental paradigm and behavioral performance

To study how behavioral relevance can shape neural representations of sensory signals in the early visual system, I designed a visual foraging task. I used a setup in which mice were head-fixed but free to move on a treadmill. Since the head was in a stable position throughout the experiments, this setup had the advantage of controlling visual input without restricting mice in their movements. Mice were trained to discriminate between two stimuli, which consisted of downward moving drifting gratings presented behind two different apertures, a square and a diamond, and differed in reward contingencies. The two stimuli were big in size (45°-55° diameter) and exceeded typical V1 receptive field sizes (10° or greater) (Hübener, 2003; Niell and Stryker, 2008) so that identical visual stimulation of recorded V1 neurons was implemented. Most of the recorded V1 neurons, whose receptive fields were located within the stimulus aperture, were therefore driven by only the identical drifting grating, whereas the whole animal could distinguish between the two different apertures and associate reward with one stimulus, but not the other. The grating would be irrelevant for the task, but allowed measurement of the response properties of the recorded neurons and testing of whether they were affected by context. After a short pause, mice could trigger a trial, and therefore stimulus onset by crossing a speed threshold of 5 cm/s for a duration of 500 ms. One stimulus ('go') promised a fluid reward which the animal could earn by running for another 4 s. If the animal ran for 4 s during the go-stimulus presentation, it was considered a hit trial. The other stimulus ('stop') did not have any consequences. If the animal ran for 4 s in response to the stop stimulus, it was considered a false alarm. In both cases stimulus presentation stopped after 4 s, and the animal could start a new trial by slowing down and starting over again. At any point in time, the animal could terminate the current trial by slowing down and immediately start over; these terminated trials were considered correct aborts if the stop-stimulus was shown, or incorrect aborts if the go-stimulus was shown (**Figure 6**A). The strengths of the behavioral paradigm are that (1) for both stimuli the animal's running behavior was identical around the time of stimulus onset, and (2) the single drifting grating provided identical sensory stimulation to those neurons whose classical receptive fields (RFs) were contained within the stimulus frame.

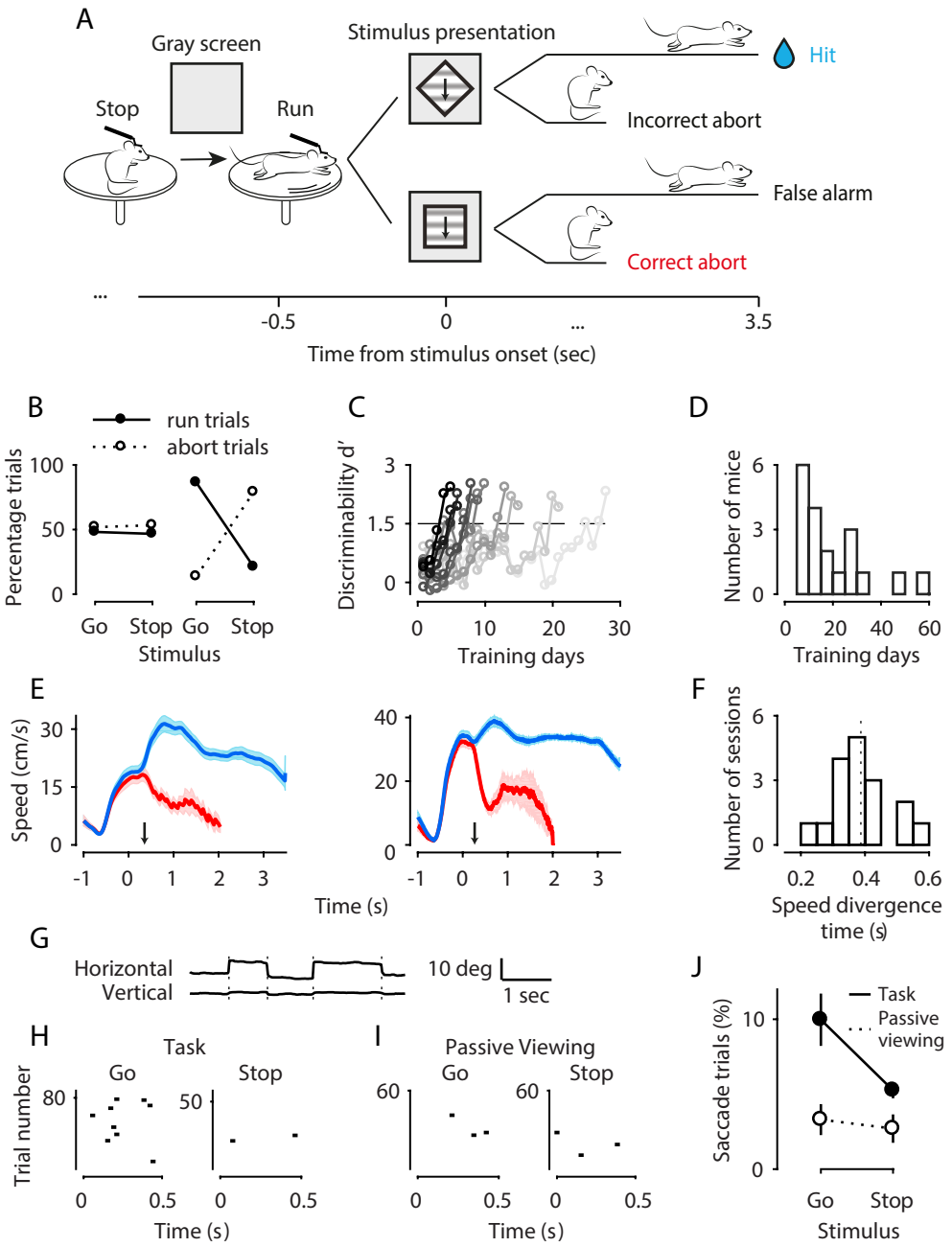

Figure 6: Experimental paradigm and behavioral performance. **(A)** Schematic of the visual foraging task. **(B)** Behavioral performance for one example mouse (M85) during an early (session 7, left) and late stage (session 28, right) of training. **(C)** Learning curves of 10 example mice. Animals were considered as trained when d' ≥ 1.5 for 2 consecutive sessions. **(D)** Summary of training sessions across the sample of mice (n = 19). **(E)** Trial-averaged run speed traces aligned to the representation of the go (blue) and stop stimulus (red), obtained in single sessions of two trained mice. Shaded area indicates ± SEM. Dotted lines mark the point in time, at which the divergence of the two traces is statistically significant (left: 355 ms; right: 265 ms). **(F)** Summary of speed divergence times across all sessions (n = 17 sessions from 8 mice). Dotted line marks mean at 387 ms. **(G)** Example traces for vertical and horizontal eye positions. Dashed lines indicate saccades. **(H)** Saccade activity across trials aligned to the presentation of the go stimulus (left), or stop stimulus (right). Markers represent detected saccades. **(I)** Same, during passive viewing. **(J)** Average percentage of saccade trials during task and passive viewing, separately for the two stimuli. Error bars are ± SEM after variability across sessions had been removed (Loftus and Masson, 1994).

After a few training sessions, mice learned to discriminate between the stimuli and earn rewards (**Figure 6**B-D). During early training stages, naïve animals typically ran on a substantial portion of trials regardless of which stimulus (go or stop) was shown (**Figure 6**B, left). Trained animals, in contrast, yielded high running rates for the go stimulus (hit trials), but terminated most of the trials when the stop stimulus was shown (correct abort trials), leading to low false alarm rates. By terminating trials in which the stop stimulus was shown, the animal saved energy and time, because the next reward could be earned faster. To quantify and track behavioral performance over days, I computed the discriminability index d' from signal detection theory (Macmillan and Creelman, 1991) (**Figure 6**C,D). The sensitivity index d' is a measure of the difference in the proportion of hit and false alarm trials and therefore gives a measure of how well the animal can discriminate between the two stimuli. Less false alarms and more hit trials lead to a higher d', and a higher d' indicates a better behavioral performance and a higher discriminability between the two stimuli. Animals were considered trained, when the d' of their behavioral performance was ≥ 1.5 for two consecutive days. Some animals reached the criterion level of d' ≥ 1.5 within few days (**Figure 6**C, dark traces), other animals needed multiple weeks (pale traces), resulting in an average of 18.9 ± 3.4 training days (mean, standard error of the mean, n = 19). Once the animals had learned the task they showed stereotypical running behavior, which reliably reflected the reward assignments (**Figure 6**E,F). Two example animals are shown in **Figure 6**E. Stimulus onset was triggered at time 0 by running above threshold for 500ms. After presentation of the go stimulus, run speed remained high until reward delivery (blue traces). In contrast, when the stop stimulus was shown, run speed dropped quickly again (red traces). Running speed has been shown to influence neuronal processing in the early visual system (e.g. Erisken et al., 2014; Niell and Stryker, 2010). Therefore, I needed to control for running behavior and for my further analyses used a time window in which running speeds did not differ between conditions. Running behavior for the go and stop stimuli was equal around stimulus onset, but changed quickly after that. I determined, for each individual recording session, the time window of stimulus presentation during which speed was indistinguishable (**Figure 6**E,F). I compiled distributions of run speeds across trials, separately for hits and correct aborts, and compared these distributions at every point in time. I took as point of speed divergence the first of three consecutive time points with significantly different speed after stimulus onset (Kolmogorov-Smirnov test, $p < 0.01$). For the two sessions shown in **Figure 6**E, running speeds were indistinguishable during the first 355 ms (left) or 265 ms (right) of stimulus presentation. Across all sessions in which I obtained neuronal data, the resulting points of speed divergence varied with an average of

387 ± 23 ms (**Figure 6**F). The time from stimulus onset to the point of speed divergence determined for every individual recording session the time window for further analyses.

During time windows of equal running speed, I analyzed eye movements and found systematic differences across stimulus conditions (**Figure 6**G-J). In addition to the foraging task experiments, I showed in a separate block of trials periodic sequences of the same stimuli unrelated to the animals' behavior. In this passive viewing condition, the rewarding spout was taken away to remove any association between the shown stimuli and reward. Therefore, in comparison to the foraging task, stimuli were behaviorally irrelevant during passive viewing experiments. In traces of horizontal and vertical eye position I identified saccadic eye movements (**Figure 6**G) in all four conditions (task: hits and correct aborts; passive viewing: square and diamond) and aligned them to stimulus onset, focusing on the periods of equal running speeds. Comparing saccade movements across stimuli and task conditions showed systematic eye movements in single sessions which reflected reward contingencies: saccadic eye movements occurred more frequently during presentation of the go stimulus, but only when the animal was engaged in the task. During the passive viewing condition eye movements were rather rare (**Figure 6**H,I). This pattern was also evident when combining all sessions (**Figure 6**J): on average, the percentage of contaminated trials was higher during the task than during the control condition (main effect of task: 7.6% vs. 3.0%, $p = 0.029$, ANOVA). During the task, but not during the control condition, the percentages of contaminated trials differed between stimuli (interaction between stimulus and task: $p = 0.044$, ANOVA). Follow-up analyses confirmed that, during the task, saccades occurred more often for the go stimulus than for the stop stimulus (10.0% vs. 5.3%, $p = 0.015$). This was not the case for the passive viewing condition, where the percentage of saccades was indistinguishable (3.3% vs. 2.7%, $p = 0.25$), indicating that these eye movements were not merely triggered by sensory properties of the stimuli. These eye movements, which most frequently appeared during task engagement and the presentation of the go stimulus, were likely to reflect the animals' reward expectancy. For further analyses, I strictly removed every trial in which a saccade occurred.

3.2 Isolating effects of behavioral relevance needs precise control over sensory input

The differences in running speed and eye position across different stimulus conditions showed that investigating how behavioral relevance might shape

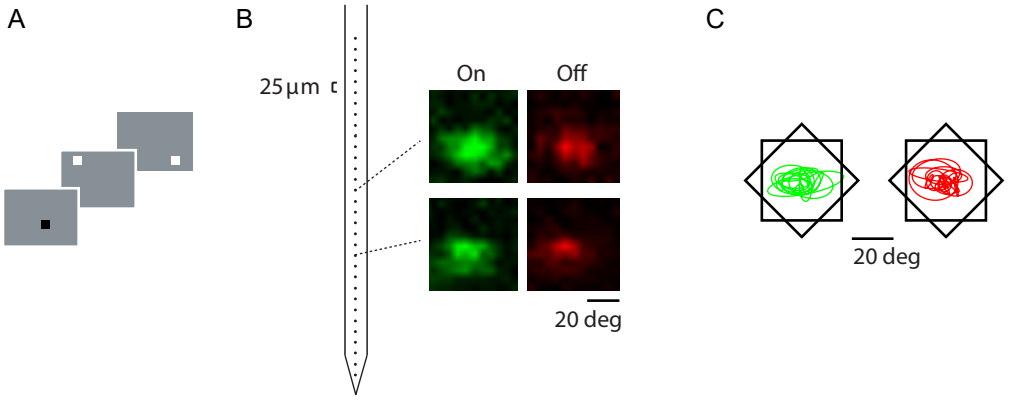

Figure 7: Measuring receptive field properties to allow precise sensory drive. **(A)** To estimate ON and OFF subfields of RF position, a sparse noise stimulus (Liu et al., 2010) was presented which consists of white or black squares (5° diameter) briefly flashed (150 ms) at random locations on a square grid (60° diameter). **(B)** Left: Schematic drawing of a 32-channel probe with electrodes spaced at 25 µm. Right: two example multiunit ON (green) and OFF (red) receptive fields from two electrodes. **(C)** RF estimates for one example session, which were obtained by fitting two-dimensional Gaussians to the maps of average firing rates, and their relative position within the two stimuli (n = 13). Colors same as in B.

responses of V1 neurons requires precise control over sensory drive (**Figure 8**). As a first step I measured receptive field locations of simultaneously recorded V1 neurons and positioned the stimuli such that they maximally overlap many RFs (**Figure 7**). The stimulus size exceeded receptive field size of several neurons; with careful positioning the recorded neurons were only driven by the downward moving drifting grating, without being influenced by the overall shape, and therefore could not distinguish between the stimuli. In contrast to monkeys, which can be trained to keep their eyes fixated throughout the trial, to my knowledge mice cannot be trained yet to keep their eyes fixated during single trials. Therefore, offline analyses of recorded eye tracking data allowed for the evaluation of eye positions after the experiments. By comparing eye positions across all four stimulus conditions, I found significant differences in the horizontal as well as vertical plane (**Figure 8**). I compared the cumulative distribution of mean trial eye positions across all four conditions (go-/ and stop-stimulus during task engagement and passive viewing), in a time window of equal running speed after removing saccade trials (**Figure 8**A-B, black traces). Their cumulative distributions were distinguishable in the horizontal as well as vertical plane as seen in the two example sessions in **Figure 8**C-D ($p < 0.01$, Anderson-Darling test). To provide identical sensory input, I then matched eye positions across all conditions. I applied, for each ensemble of simultaneously recorded neurons, for the time window of identical running speed a stratification procedure

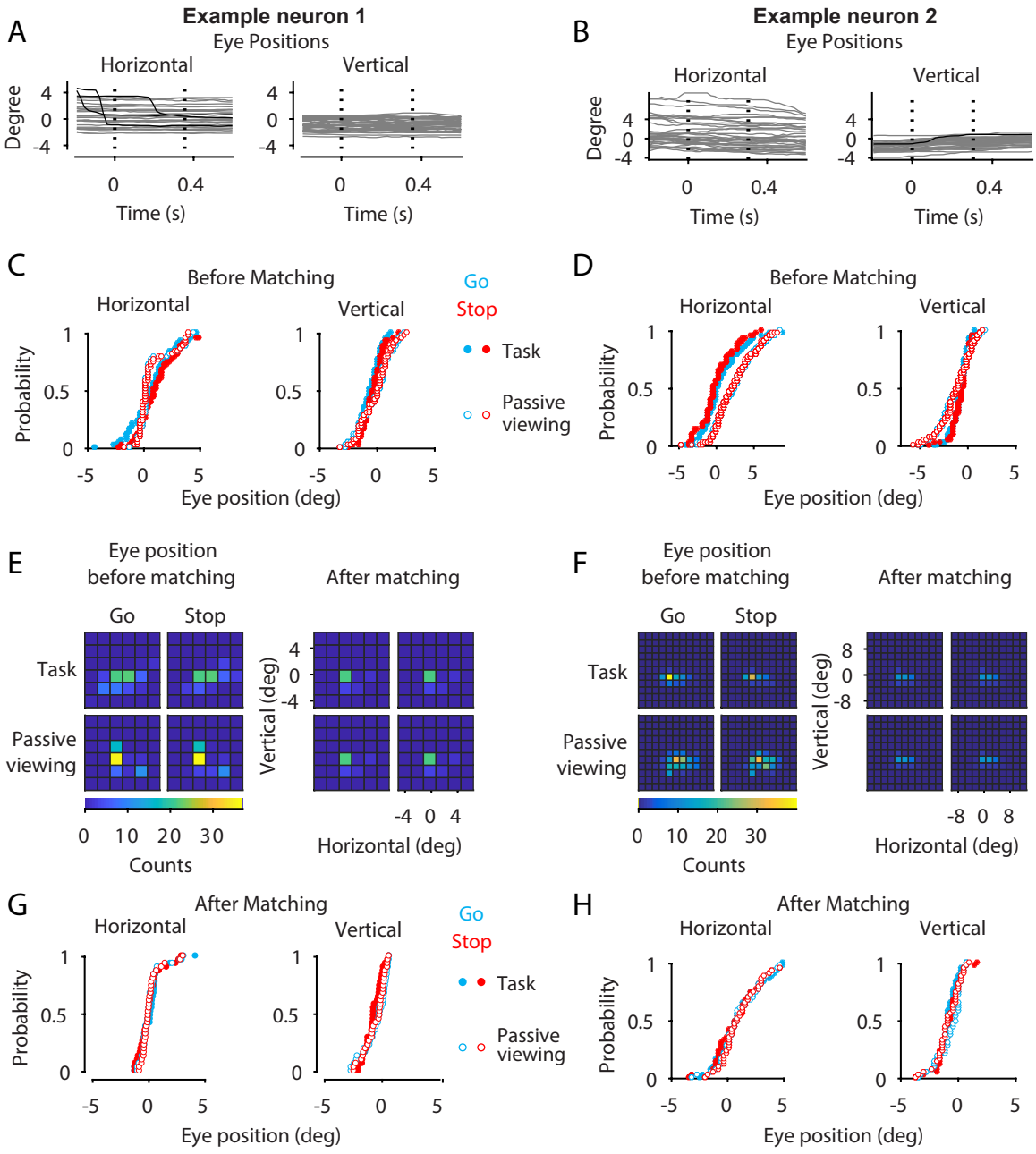

Figure 8: Matching of eye positions across different stimulus conditions. **(A)** Single trial horizontal (left) and vertical (right) eye positions during task condition aligned to stimulus onset for one example session. First dotted line indicates stimulus onset, second: time point of speed divergence. **(B)** Same as A, for a second example session. **(C)** Cumulative density function of horizontal (left, $p < 0.0001$) and vertical (right, $p < 0.0001$) eye position for all four stimulus conditions for one example session. Filled dots, task; empty dots, passive viewing; cyan dots, go stimulus; red dots; stop stimulus. **(D)** Same as C, for a second example session. Left, $p < 0.0001$; Right, $p < 0.0001$ **(E)** 2-D histogram of eye position before (left) and after (right) matching procedure during task (upper row) and passive viewing (lower row) condition. Each square represents a 2-degree bin of horizontal and vertical eye position counts. **(F)** Same as E, for a second example session. **(G)** Cumulative density function of horizontal (left, $p = 0.8$) and vertical (right, $p = 0.4$) eye position for all for stimulus conditions after matching procedure. Filled dots, task; empty dots, passive viewing; cyan dots, go stimulus; red dots; stop stimulus. **(H)** Same as G, for a second example session (left, $p = 1$; right, $p = 0.4$).

(Roelfsema et al., 1998) (**Figure 8**E-F). From all trials which did not contain any saccades, I constructed 2D-histograms of time-averaged eye positions, separately for each task and passive viewing stimulus condition (**Figure 8**E-F, left). In each position bin, the number of trials was matched by finding the minimum number across conditions and removing, where necessary, excess trials from the other conditions (**Figure 8**E-F, right). To confirm that the matching procedure removed any differences in eye positions I compared again after the stratification procedure, without binning, their cumulative distributions across all four conditions and found that they were indistinguishable (**Figure 8**G-H, G: horizontal position: $p = 0.77$; vertical position: $p = 0.36$; H: horizontal position: $p = 0.98$; vertical position: $p = 0.4$; Anderson-Darling test). Applying this procedure to the entire data set I found, before matching, systematic differences between the cumulative distributions in every single session (**Figure 9**, left, $n = 33$). In 12 sessions obtained from 5 mice, I could completely match all eye positions (**Figure 9**, right, all $p > 0.1$); I focused on those sessions only for the analyses of neural data from V1.

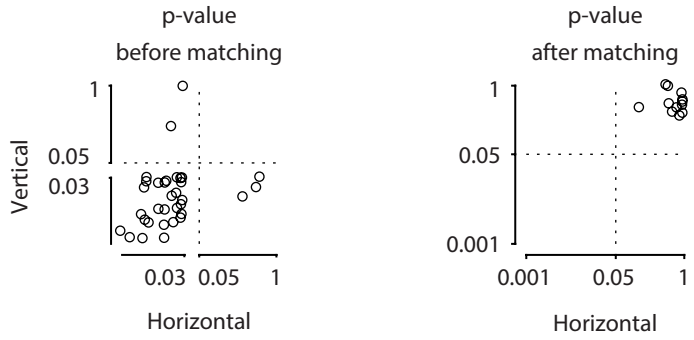

Figure 9: Summary of statistical tests for eye position matching, as shown in **Figure 8**E-F. Left, p-values of the comparison of eye position distributions from all four conditions before matching (Anderson-Darling-Test). Each data point represents p-value of horizontal and vertical eye position comparison of one recording session ($n = 33$). Right, same after eye position matching ($n = 12$).

3.3 Neurons in V1 can reflect stimulus identity during task engagement

After carefully controlling for the sensory drive, I found that a substantial fraction of V1 neurons could discriminate between the stimuli during task engagement. First, I wanted to make sure that recorded V1 neurons indeed could not discriminate between the stimuli in the passive viewing condition (**Figure 10**A-D, left panels). I quantified discriminability, by separating single-trial firing rates evoked by go versus stop stimuli and asked how well an ideal observer could decode stimulus identity. In both example neurons shown in **Figure 10** (A,C,left) firing rates were indistinguishable for both stimuli and the area under the receiver operating characteristic (ROC) curve (AUROC) was not significantly different from chance performance (**Figure 10**B,D, left panels, AUROC = 0.53 and 0.46, $p > 0.01$, randomization test). During task performance, however, both neurons could reliably discriminate the stimuli. The first example neuron showed a higher firing rate to the go than to the stop stimulus and the area under the ROC curve was significantly different from chance performance (**Figure 10**A,B, right panels, AUC = 0.68, $p = 0.01$, randomization test). The second example neuron showed the opposite effect with a stronger response to the stop stimulus (**Figure 10**C,D, right panels, AUC = 0.29, $p = 0.01$, randomization test). Insets in **Figure 10**A,C (middle) show spike waveforms of each neuron obtained throughout the recording session. The waveforms are essentially identical, showing that the neuron was held long enough to record its activity during task and passive viewing conditions.

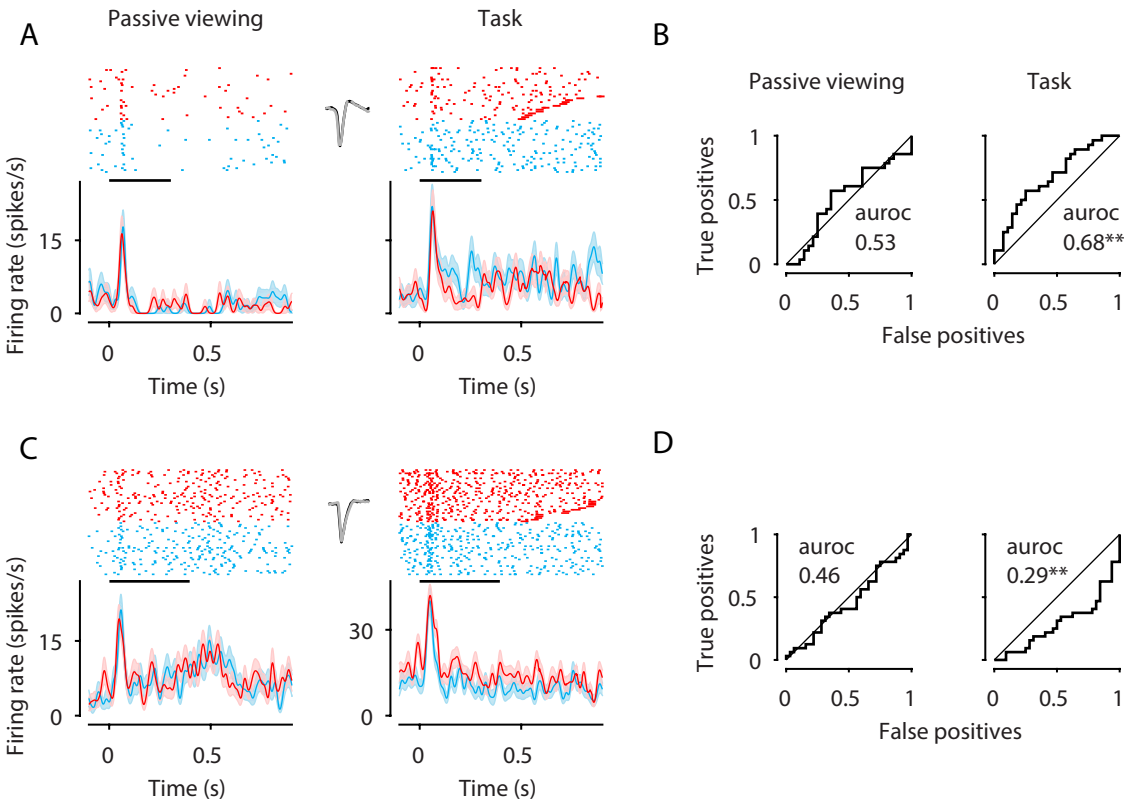

Figure 10: Responses of V1 neurons can reflect behavioral relevance. **(A)** Spike rasters (top) and spike density function (bottom) of responses aligned to stimulus onset for one example neuron during passive viewing (left) and task engagement (right). Red, stop stimulus. Cyan, go stimulus. Small inset (middle) shows spike wave shapes during left (black) and right (gray) blocks of trials. Black bar, time window of identical running speed (see **Figure 6**E-F). **(B)** ROC curves for firing rates in A with auroc (area under ROC curve) values, left during passive viewing, right during task engagement. The two asterisks indicate that the auroc value is significantly different from chance level (p = 0.01) **(C)** Same as A for second example neuron. **(D)** ROC curves same as in B for example firing rates in C.

By testing the whole population of recorded V1 neurons for task dependent modulations, I found that a substantial fraction reliably discriminated between the stimuli during task engagement (**Figure 11**). Out of 168 neurons that could not discriminate between stimuli during passive viewing (**Figure 11**), 25% (n = 42) showed differences in response strengths to the go and stop stimuli during task engagement and therefore reliably signaled the identity of the stimulus (blue and red data points). One half of the group showed a stronger response to the go stimulus (12.5%, shown in blue), while the other half responded stronger to the stop stimulus (12.5%, shown in red) (**Figure 11**). Summarizing these data shows that neuronal processing in the mouse primary visual cortex can be influenced by behavioral context. Neurons, which showed the same response to identical stimuli during passive viewing, became selective during task engagement.

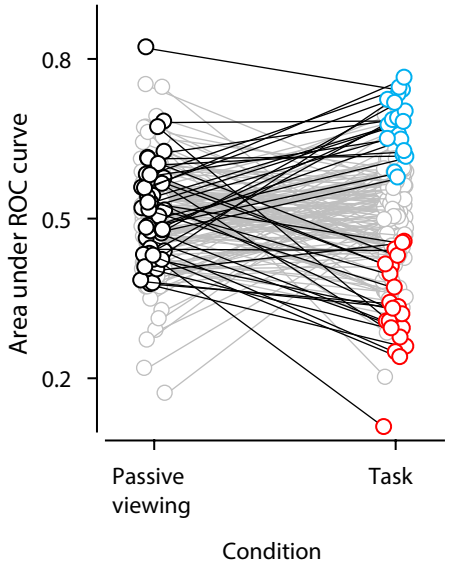

Figure 11: A substantial fraction of V1 neurons encode stimulus identity during task engagement. Summary for all cells (n = 168). Values for area under ROC curve during passive viewing and task condition. Grey and black color, area under ROC curve not significantly different from chance performance. Blue and red color, area under ROC curve is significant (n = 42). 12.5% showed higher firing rate for go-stimulus (blue, n = 21), 12.5% showed higher firing rate for stop-stimulus (red, n = 21) during task performance. The value 0.5 indicates chance performance.

3.4 Effects of behavioral relevance of stimuli in dLGN are rare

Context dependent changes in neuronal firing rates could either be a cortical phenomenon or be inherited from subcortical structures. The main input to V1 consists of projections from the dLGN, which is affected by behavioral state (Erisken et al., 2014) and attention (McAlonan et al., 2008; O'Connor et al., 2002). Therefore, the dLGN could transmit information about behavioral context to its downstream targets. In contrast, if the modulations we observed in V1 neurons were created in cortex, we should not observe them at the level of the thalamus. To test this hypothesis, I recorded from the dLGN during the same visual foraging task (**Figure 12**). Recordings from this deeper structure in the brain can be verified by a combination of criteria like typical receptive field progression (**Figure 12**, left) and recording depth.

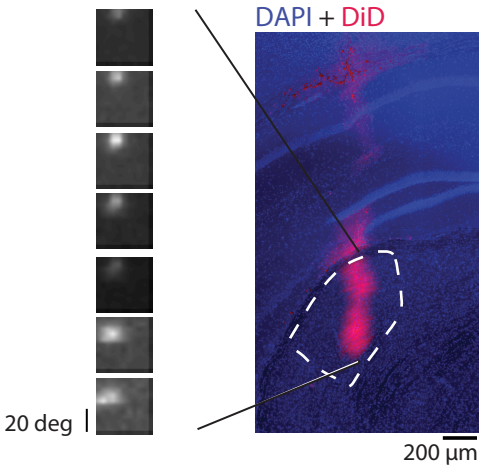

Figure 12: Example recording from dLGN. Left, receptive field progression based on multiunit activity on neighboring electrodes on the linear probe. Right, coronal section of the brain, the dLGN is marked by the white outline. DAPI shown in blue; electrode was coated with DiD and the trace is shown in magenta.

To our dataset of recorded dLGN neurons I applied the same analyses as for V1 neurons, including the control of visual input by matching eye positions, and asked whether stimulus representation changes during task engagement. Most dLGN neurons did not encode stimulus identity and showed similar responses to both stimuli during passive viewing (**Figure 13**A,B, left, AUC = 0.55, $p > 0.05$, randomization test) as well as during task performance (**Figure 13**A,B, right, AUC = 0.53, $p > 0.05$, randomization test). Only a small subset of neurons encoded stimulus identity during task performance, as seen in the example neuron in **Figure 13**C-D. For this neuron, during passive viewing both stimuli were indistinguishable (**Figure 13**C-D, left, AUC = 0.43, $p > 0.05$, randomization test), but showed solid discrimination during task performance (**Figure 13**C-D, right, AUC = 0.29, $p < 0.01$, randomization test). As before, the neurons could be held throughout the recording session as the waveforms from both experiments are essentially identical.

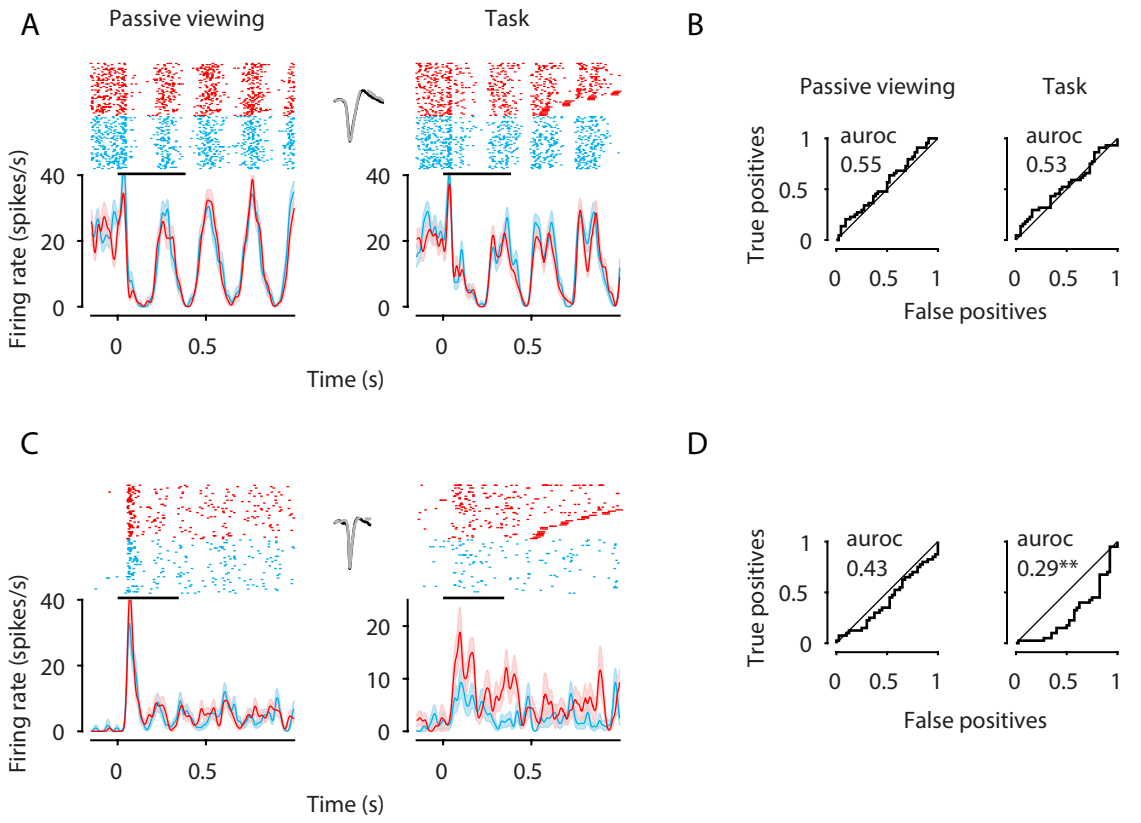

Figure 13: Few dLGN responses reflect stimulus identity. **(A)** Spike rasters (top) and spike density function (bottom) of responses aligned to stimulus onset for one dLGN example unit. Black bar, time window of same running speed (see **Figure 6**E-F). Left, passive viewing. Right, task engagement. Middle, Inset shows spike waveforms during task and passive viewing experiments. Black and grey correspond to left and right block of trials, respectively. **(B)** ROC curves comparing distributions of firing rates for the task (left) and passive viewing (right) condition. **(C-D)** Same as A-B for second dLGN example neuron. Red in A and C: stop stimulus. Cyan: go stimulus.

In the population of 48 recorded dLGN neurons which did not discriminate between stimuli during passive viewing, only five (10%) showed improved discrimination during task performance (**Figure 14**). One neuron responded more strongly to the stop stimulus and four showed a higher firing rate when the go stimulus was present (**Figure 14**, shown in red and blue, respectively). The proportion of neurons modulated by stimulus context was lower in area dLGN than in V1 (10% in dLGN versus 25% in V1, p = 0.03, Kolmogorov-Smirnoff test). Taken together, these data show that discriminability is less present in dLGN than in V1 and suggests that these effects are amplified, if not created, in cortex.

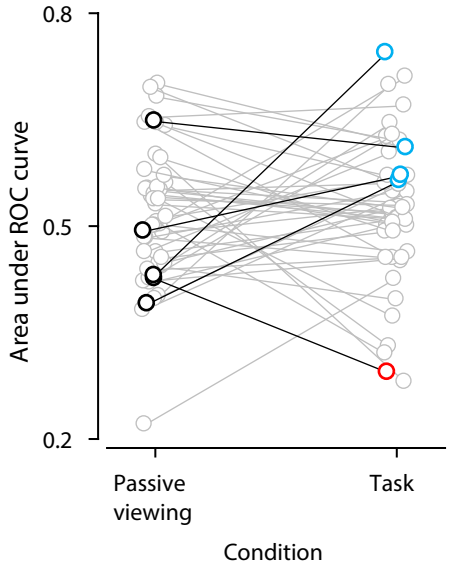

Figure 14: Summary of discrimination strength of dLGN neurons during passive viewing and task engagement. Values for area under ROC curve during passive viewing and task condition (n = 48). Grey and black: area under ROC curve not significantly different from chance performance. Blue and red: area under ROC curve is significant (n = 5, 10%). 8 % of neurons showed higher firing rate to the go stimulus (blue, n = 4), 2 % showed higher firing to the stop stimulus (red, n = 1) during task performance. The value 0.5 indicates chance performance.

3.5 Contribution of different cell classes to task dependent discrimination

Knowing that stimulus context can shape response properties in mouse V1, I further wanted to investigate the underlying circuit mechanisms and tested the role of intracortical inhibition. Mouse genetics offers the possibility to target specific cell types to gain insights into circuit mechanisms. If inhibitory interneurons indeed play a special role, I would predict to find stronger modulations in the subpopulation of putative inhibitory neurons. To test this hypothesis, I investigated how interneurons, of which the most common type are PV+ interneurons (Gonchar and Burkhalter, 1997), are involved in context dependent modulation in comparison to excitatory neurons. A larger goal would be to investigate all three subtypes of interneurons, but VIP+ and SOM+ neurons are rare and therefore difficult to identify with the electrophysiological methods used in this work. To identify PV+ neurons in my recorded population, I performed optogenetic tagging experiments after expressing the light-sensitive cation channel ChR2 selectively in PV+ interneurons of a PV-Cre mouse strain (**Figure 15**A-B). Furthermore, I clustered V1 neurons into two groups according to their extracellular waveform: narrow-spiking neurons, corresponding to putative fast-

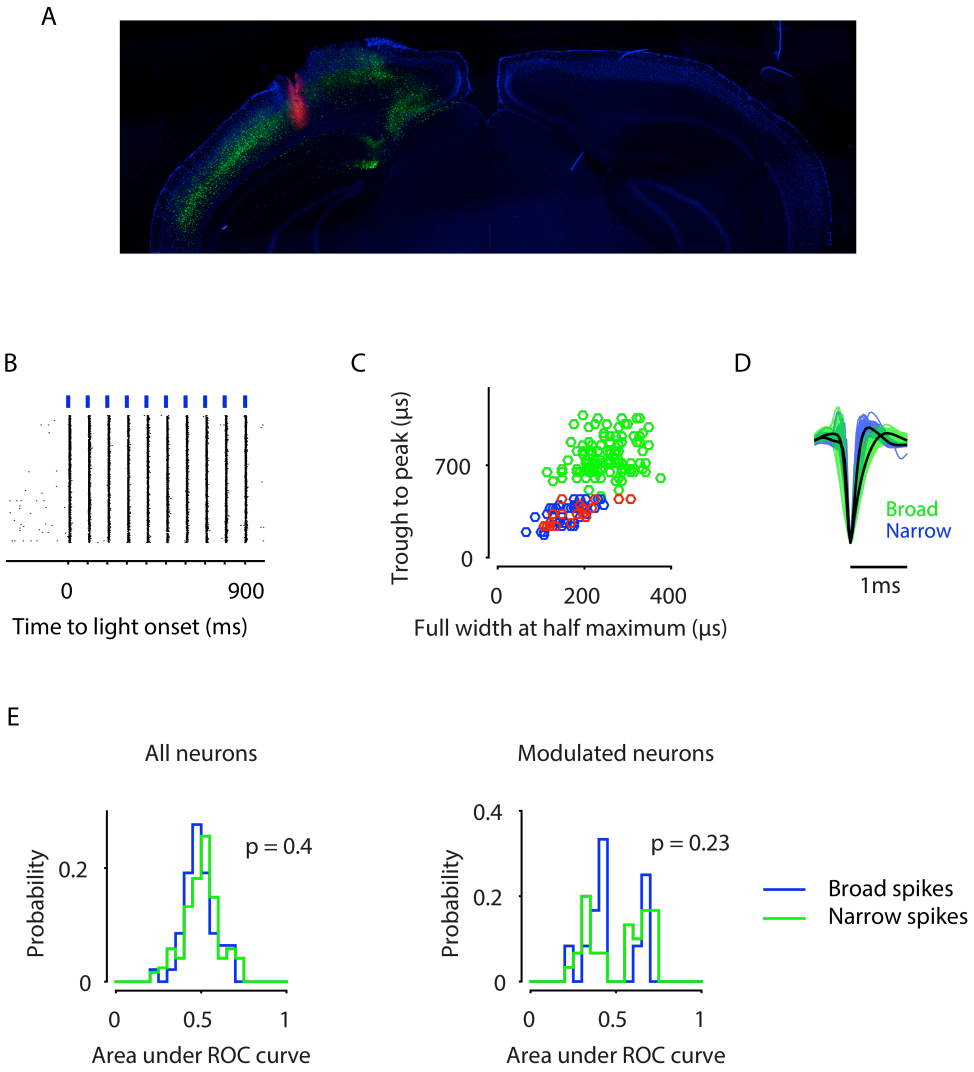

Figure 15: Optogenetic tagging and comparison of task dependent effects within different cell classes**. (A)** Coronal section of mouse brain. Blue, DAPI; green, eGFP (indicating virus expression); red, DiD indicating electrode trace **(B)** Raster plot showing PV+ tagging of one example neuron, aligned to the beginning of a train of light pulses. Blue ticks represent 1 ms blue light pulses at 10 Hz. **(C)** Clustering of recorded V1 population into broad-spiking (green, n = 121) and narrow-spiking (blue, n = 47) neurons, with tagged PV+ interneurons (n = 22) highlighted in red. **(D)** Normalized waveforms from both narrow- and broad-spiking neural clusters (blue and green, respectively). Black lines represent average waveform for each group. **(E)** Left: Histogram of ROC values from all recorded V1 neurons, divided into broad- (n = 121, white) and narrow-spiking (n = 47, grey) cells. Right, same for subset of neurons which showed significant modulation by stimulus context (grey, n = 12; white, n = 30) (see **Figure 11**).

spiking inhibitory interneurons, and broad-spiking neurons corresponding to putative excitatory neurons (**Figure 15**C-D). The group of tagged PV+ interneurons overlapped with the cluster of narrow spiking waveforms, therefore verifying that this cluster represents putative inhibitory interneurons. Of the V1

population (n = 168), 28 % of neurons (n = 47) constituted the group of narrow-spiking neurons, while the rest (78 %, n = 121) fell in the group of broad-spiking neurons (**Figure 15**C). **Figure 15**D shows the mean waveforms for all recorded neurons. After separating the population of recorded V1 neurons into two cell classes, I examined whether context dependent modulation differed between them. In the whole population, modulation strength across both cell classes did not show any differences (mean AUROC deviation from chance level (0.5), narrow spiking = 0.07, broad spiking = 0.08, p = 0.4, Kolmogorov-Smirnoff test) (**Figure 15**E, left). Considering only the subset of neurons which were significantly modulated by stimulus context (see **Figure 11**) revealed that 25 % of broad-spiking (n = 30 out of 121) and 26 % of narrow-spiking (n = 12 out of 47) neurons were affected, therefore building nearly the same fraction of modulated neurons from both classes (**Figure 15**E, right). The modulation strength of modulated neurons between these two classes showed no differences as well (mean AUROC deviation from chance level: broad spiking = 0.16, narrow spiking = 0.14, p = 0.23, Kolmogorov-Smirnoff test) (**Figure 15**E, right). Taken together, across the whole V1 population, putative interneurons seem to match activity from putative excitatory neurons, by showing similar modulation strength and building the same fraction of neurons which are significantly modulated by behavioral relevance. The subpopulation of significantly modulated neurons showed as well the same effects with similar modulation strengths across both cell classes. The group of narrow-spiking cells is presumably mostly represented by PV+ interneurons, suggesting that PV+ interneurons might play a role in task dependent modulations, but rather reflect network activity of putative excitatory neurons.

4 Discussion

In this thesis, I investigated how behavioral relevance can influence sensory processing in the early visual system of the mouse. To approach this question, I designed a visual foraging task, in which I used two stimuli, which provided identical sensory stimulation to V1 neurons but differed in reward contingencies. When mice showed stable task performance, I performed extracellular electrophysiological recordings from area V1 and dLGN. After controlling for behavioral measures including running speed and eye position, I found that a substantial fraction of V1 neurons, which could not discriminate the two stimuli during passive viewing, reflected reward contingencies during task engagement. Of the recorded V1 population, 25 % of neurons signaled stimulus identity during task performance, of which one half showed a higher firing rate when the stimulus signaling an upcoming reward was shown, while the other half fired more in anticipation of the other stimulus. These findings are consistent with the idea that V1 sensory processing can depend on the behavioral relevance of a stimulus. To test whether these context dependent modulations are inherited from the thalamus, I performed recordings from the dLGN. In contrast to V1, recordings from dLGN during the same task revealed that neuronal modulation due to behavioral relevance is less evident. Only 10 % of the recorded dLGN neurons signaled stimulus identity, which suggests that modulatory effects influence an increasing number of neurons when ascending the visual processing hierarchy. In addition, I investigated the underlying circuits in the cortex by testing the role of putative inhibitory interneurons in context dependent modulations. I found that the strength of task dependent modulation of putative inhibitory interneurons was similar compared to putative excitatory neurons. The observation of modulatory influences on V1 neuronal activity in the mouse might provide the basis for investigating how top-down influences modulate sensory processing.

4.1 Choice of behavioral paradigm

The goal to understand how behavior influences neural circuits has been investigated in a large body of literature obtained with macaque monkeys engaged in complex behavioral tasks. As in spatial attention studies, differences in firing rates across different task conditions allow correlation of neural activity with behavior. These studies stand out for their precise control over several behavioral measures, and identical sensory drive during different task conditions. In developing a visual foraging task for the mouse, I attempted to reproduce some of

the key properties of these standards. For example, monkeys need to actively initiate a trial by keeping their eyes fixed on a fixation point on the monitor. This feature ensures an active state at every trial start and allows attribution of error trials to perceptual or decision errors. In the visual foraging task presented in this work, trial initiation occurred by first stopping for a short time, and then starting to run again for 500 ms. When mice were highly motivated, they were able to perform around 400 trials within 40 minutes. Once they were satiated and motivation dropped, I observed them mostly remaining stationary. In this case, no trial initiation occurred, and I continued with passive viewing experiments. In a classical conditioning paradigm, in comparison, the animals' motivation and attention might fluctuate during the behavioral task and results can be contaminated with error trials. For example, over the course of a training session the animal's motivation might decrease and therefore stimuli are less likely detected, which could lead to the incorrect conclusion that the ability to detect a stimulus has diminished.

When linking neural activity in sensory areas to behavioral context, it is important to keep the sensory input to neurons of V1 and dLGN identical. In my paradigm, I achieved this goal by choosing two similar stimuli, which differed only in shape. Both stimuli contained a downward moving drifting grating and exceeded the classical receptive field size of neurons, such that with a careful positioning most of the recorded neurons were driven by the same sensory stimulation. Therefore, recorded neurons in mouse V1 would only 'see' the drifting grating and could not discriminate between the two stimuli during passive viewing, whereas the whole animal was able to associate reward with one stimulus, but not the other, during task engagement. In this way, it was possible to isolate effects of task engagement on sensory processing of identical stimuli.

As a last point it was important to control for the behavioral output with which the animal signals its decision. In case of the visual foraging task presented in this work, mice reported their choice by running speed, a behavior which can influence cortical and subcortical visual activity (e.g. Erisken et al., 2014; Niell and Stryker, 2010). To isolate effects of task dependent changes on sensory processing, I needed to control for the running behavior, since effects of locomotion could confound the effects of context modulation. To keep running behavior identical, I determined for every individual session the time window after stimulus onset in which running speeds were the same.

Taken together, the behavioral paradigm used in this work is well suited to investigate how behavioral relevance of a stimulus shapes neural activity by (1) using active trial initiation to ensure high motivation levels during task

performance, (2) providing identical sensory input to recorded V1 and dLGN neurons, and (3) controlling for the running behavior by having a time window of equal running speed after stimulus onset.

Complex visually guided behaviors in a head-fixed setup require training times in a range from a few days (Poort et al., 2015; Sanders and Kepecs, 2012) to several weeks and months (Andermann, 2010; Burgess et al., 2017; Glickfeld et al., 2013b; Guo et al., 2014; Mayrhofer et al., 2013; Pinto et al., 2013; Wekselblatt et al., 2016). The average training duration for the discrimination task in this work was 19 days and is therefore at the lower range of training times among different task approaches.

4.2 Control of eye movements

To assign small changes in firing rates during task performance to modulation by stimulus context, one needs to carefully control for the sensory input. One way is to use identical stimuli, as described above. Additionally, since eye movements through saccades and even microsaccades can change neuronal responses to a stimulus through a bottom-up process (e.g. Leopold and Logothetis, 1998; Wurtz, 1969), it is important to keep eye positions constant when isolating behavioral correlates in neural processing. To my knowledge, mice have not yet been trained in an eye fixation paradigm. However, even when monkeys maintain fixation during task performance small differences in eye position can still occur (Hafed and Clark, 2002; Hafed et al., 2011; Roelfsema et al., 1998) and need to be controlled for offline. In this work I found differences in eye positions and movements when mice were engaged in a task versus the passive viewing condition. Although the mouse retina exhibits no specialized central vision as in a fovea (Jeon et al., 1998), other studies have mentioned as well that eye movements occur more frequent when mice are running in comparison to being mostly stationary (Ayaz et al., 2013; Erisken et al., 2014; Jurjut et al., 2017; Keller et al., 2012; Poort et al., 2015). This behavior may help to collect more information about the surrounding world while being active (Chen et al., 2015), or may simply help to refresh the image on the retina (Pritchard, 1961).

In addition to these differences I found that during task engagement, saccades occurred more frequently when the stimulus signaling an upcoming reward was presented (hit trials). If a stimulus is associated with high reward it more likely leads to a saccadic eye movement towards that stimulus than towards that very same stimulus associated with low reward (Theeuwes and Belopolsky, 2012). In the saccadic eye movement circuitry in primates, the lateral intra-parietal area

(LIP) is thought to transform visual signals into eye movement commands. Neurons in the LIP respond in a graded manner to both the amount of expected reward, and the probability of a reward before execution of the response (e.g. Glimcher, 2003; Platt and Glimcher, 1999). In goal directed behavior, these eye movements might be crucial for linking fixation patterns to task demands, leading to more eye movements when a stimulus associated with a reward is present. Nevertheless, a similar circuitry has not been investigated in rodents. Additionally, eye movements in rodents don't seem to be specialized for fixating objects, rather they help to generate an overhead view that helps for predator detection as has been shown in rats (Wallace et al., 2013).

4.3 Task dependent modulation in sensory processing

Tracking the same neurons during task engagement and passive viewing experiments allowed for the investigation of rapid changes in sensory processing when stimuli became behaviorally relevant. The representation of identical stimuli during passive viewing changed during task engagement towards a higher discriminability of the two stimuli. Since I analyzed neuronal data in a time window of equal running speed, and in this window matched eye positions, this discriminability was not contaminated by differences in motor activity (e.g. Erisken et al., 2014; Niell and Stryker, 2010). Sensory processing in mouse V1 has been shown to be influenced by learning (Jurjut et al., 2017; Poort et al., 2015), as well as task engagement when animals where engaged in discrimination tasks of different modalities (Poort et al., 2015). Additionally, in monkeys neuronal firing rates in V1 can be influenced by reward expectancy (Stănişor et al., 2013), what has been shown in rats as well even in the absence of visual stimulation (Shuler and Bear, 2006). Consistent with previous findings the results presented in this work provide evidence that non-sensory signals directly influence sensory processing, presumably through top-down effects, and might help to improve the readout of important stimuli to downstream targets as described before in monkey studies (e.g. Buffalo et al., 2010; Ito and Gilbert, 1999; McAdams and Maunsell, 1999; Moran and Desimone, 1985; Roelfsema et al., 1998). This suggests that task engagement exerts similar effects on sensory cortex in rodents and primates.

Context dependent cortical changes of neuronal firing rates could either be driven by top-down modulation or be inherited from projections from subcortical structures. Consistent with other studies which described task or state dependent modulations in the subcortical structure dLGN (Erisken et al., 2014; McAlonan et al., 2008; O'Connor et al., 2002; Wimmer et al., 2015), I found that a small subset of dLGN neurons signaled stimulus identity during task engagement. Similar to

primates (Buffalo et al., 2010), the modulatory effects described in this work recruited more neurons when going up visual processing stages, as V1 showed a larger proportion of neurons which were affected by stimulus context than the dLGN (25% versus 10% of neurons in each area, respectively). In this context it is important to mention, that the sample size of recorded dLGN neurons in this work is small. More data from dLGN could more accurately describe the amount and strength of neurons being affected by stimulus context which in the end could be similar to those effects described in V1. What could be the underlying circuits? The thalamus receives inputs from higher cortical brain areas, including the PFC (Wimmer et al., 2015). Task dependent changes in dLGN activity might therefore be relayed to the cortex, where effects are amplified by intracortical circuits. Another possibility is that context dependent effects arise in cortex and feedback projections from cortical layer six (L6) affect firing rates in dLGN through corticothalamic feedback. Indeed L6 cortical neurons, which project vertically in the cortical column as well as project back to the thalamus, have been shown to control cortical gain largely by intracortical circuits additionally to affecting dLGN neurons through feedback activity (Olsen et al., 2012). L6 neurons receive feedback projections from higher brain areas including the anterior cingulate cortex (ACC) (Zhang et al., 2014) and could therefore influence the gain of visual responses within the cortex, as well as modulate neuronal activity in the dLGN through corticothalamic feedback projections. In all, dLGN activity seems to be influenced by nonsensory sources during task engagement and shows that context dependent modulation of sensory processing in the mouse might not only be a cortical phenomenon, although it is to mention that the small sample size might bias these results.

4.4 Potential sources of task dependent modulation

The mouse primary visual cortex receives input from subcortical structures including the dLGN and superior colliculus, but also higher order brain areas which execute cognitive functions. Several brain areas have been tested in the context of top-down modulation and each of the studies provides a possible mechanism of how nonsensory activity shapes neuronal processing for the purpose of selection. The anterior cingulate cortex (ACC) is one area which has been tested in the context of task dependent modulations. Optogenetic activation of the ACC during a discrimination task showed improvements in task performance (Zhang et al., 2014). Furthermore, activating long-range projections from ACC to V1 showed distinct changes in local circuits through innervation of different subtypes of GABAergic interneurons. Additionally, cholinergic projections from the basal

forebrain have been shown to modulate V1 processing through long-range projections. As before, activating the basal forebrain showed improvements in performance in a visual discrimination task (Pinto et al., 2013). Besides, the same structure might be implicated in rendering neurons sensitive for the timing of reward (Chubykin et al., 2013). In primates, the influence of the neurotransmitter acetylcholine in task dependent modulations of sensory processing has been tested as well (Herrero et al., 2008). Attentional modulation in V1 was enhanced after application of low doses of acetylcholine, whereas applying a muscarinic antagonist resulted in a decrease of these effects. Another study suggests that top-down modulation could be maintained by the retrosplenial cortex (RSC), which innervates layer 2/3 neurons in V1 via long-range projections and has been shown to increase its activity during learning (Makino and Komiyama, 2015). Besides direct innervation of V1 neurons, other pathways may also contribute to top-down modulation including indirect pathways through subcortical structures including dLGN or the pulvinar (McAlonan et al., 2008; O'Connor et al., 2002; Purushothaman et al., 2012). In principle these studies present possible mechanisms of how cortical areas might interact with early sensory areas to optimize the readout of sensory signals. Each of these potential mechanisms might influence V1 activity during the visual foraging task used in this work.

4.5 Does the anterior cingulate cortex show task dependent activity?

The function of the anterior cingulate area has been associated with motivation and reward-based decision making (Shenhav et al., 2016) and could therefore be a likely candidate to influence sensory processing in top-down modulation. In the mouse, ACC innervates V1 through long-range feedback projections (Zhang et al., 2014). In anesthetized as well as awake animals, ACC axon terminal activation in V1 showed innervation of local inhibitory circuits in a center-surround profile. To test if these changes help to improve the readout of visual stimuli, the group of Zhang et al. additionally trained mice in a visual discrimination task and applied laser stimulation to the ACC. During task performance, activation of the ACC resulted in improved discriminability. Nevertheless, this experiment could not show that the improved discriminability arises from direct innervation of the ACC on local V1 networks as ACC activation could improve behavioral performance through indirect pathways. Furthermore the study did not show, that ACC activity is modulated by stimulus context. If the ACC contributes to the modulation of responses in V1, we should observe task-dependent modulation of firing rates in

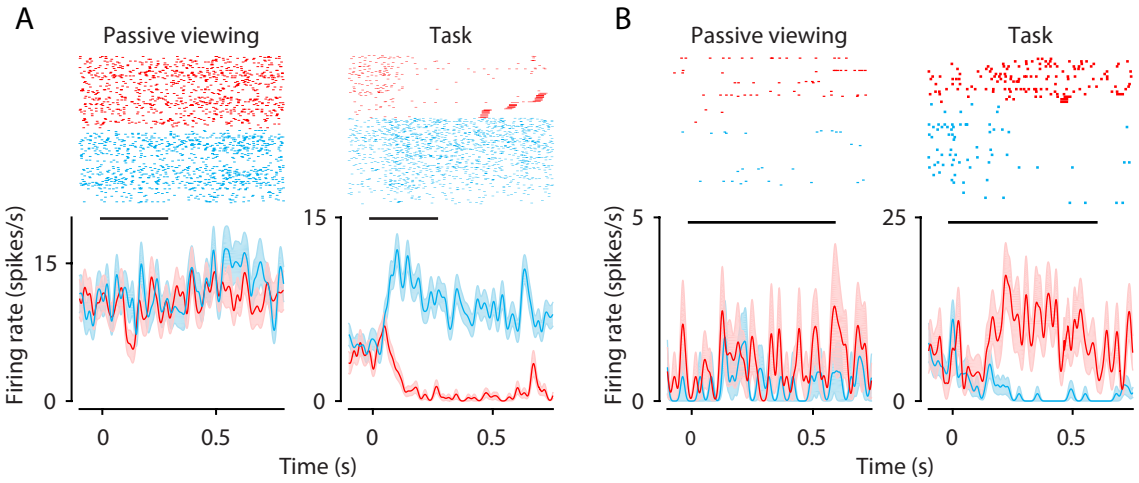

Figure 16: Task dependent changes in firing rates of ACC neurons. **(A)** Spike rasters (top) and spike density functions (bottom) of responses aligned to stimulus onset for one example neuron during passive viewing (left) and task engagement (right). Red, stop stimulus. Cyan, go stimulus. Black bar, time window of identical running speed (see **Figure 6**E-F). **(B)** Same as A for second example neuron.

ACC neurons. To test this hypothesis, I tested how activity in the ACC is influenced by stimulus context during the discrimination task used in this work. I performed electrophysiological recordings from neurons in the ACC, during the same visual foraging task, to test if activity changes when stimuli became behaviorally relevant. Preliminary data indeed demonstrated that neuronal activity was strongly influenced by stimulus context (**Figure 16**). The two example neurons in **Figure 16** showed no differences in firing rates during passive viewing (A and B, left), but strong differences in firing rates during task engagement (A and B, right). The effects in one example neuron (**Figure 16**A) were even bidirectional, with firing rates increasing when the go stimulus appeared and decreasing when the stop stimulus was shown. In this dataset of recorded ACC neurons eye position recordings were not carried out. Therefore, careful quantification of modulation effects as was done with data from V1 and dLGN was not possible. These preliminary data demonstrate that ACC signals behavioral relevance in the context of the visual foraging task used in this work and will be a promising target of further investigations of how top-down modulation influences sensory processing.

4.6 The role of interneurons in task dependent modulations

With optogenetic tagging, I identified PV+ interneurons and validated the identification of putative inhibitory interneurons in my recorded V1 population. Within the groups of nonoverlapping interneurons, PV+ cells account for a large

proportion of interneurons (40%) and are therefore mostly represented in the cell cluster of putative inhibitory interneurons (Gonchar and Burkhalter, 1997). Between the two groups of putative inhibitory and excitatory neurons, the strength of discriminability of the two stimuli during task engagement showed no differences. This result is consistent with findings in a primate attention study, where putative interneurons showed no difference in relative modulation strength in comparison to putative excitatory neurons (Mitchell et al., 2007). Additionally, in the group of significantly modulated neurons, activity of putative inhibitory neurons showed similar modulation strength to, and therefore matched the activity of putative excitatory neurons. Indeed, SOM+ and VIP+ interneurons, rather than PV+, have been shown to influence neural activity in task dependent local gain control (Makino and Komiyama, 2015; Zhang et al., 2014), which was induced through long-range top-down projections. Given the narrow extent of VIP+ neuron dendrites (Prönneke et al., 2015), their recruitment can mediate spatially localized sites of disinhibition. In this context, Karnani et al. proposed a mechanism by which PV+ and SOM+ neurons provide a 'blanket of inhibition', in which VIP+ neurons appear to allow local changes in sensory processing and might therefore be responsible for gain control (Karnani et al., 2014). Furthermore, the dense anatomical as well as functional connectivity between excitatory and PV+ neurons implies that PV+ neuron activity depends less on sensory or nonsensory input, but rather reflects local network activity (Hofer et al., 2011)

Besides, some articles reported that PV+ neuron activity might serve as a gating mechanism by enhancing feedforward functional connectivity and therefore allowing a better transformation of sensory signals into motor outputs (Atallah et al., 2012; Hamilton et al., 2013; Sachidhanandam et al., 2016). In the study from Sachidhanandam et al., PV+ neurons showed decreased activity during hit trials in comparison to miss trials in a detection task. In this study no trial initiation through the animal occurred and decreased activity of PV+ neurons might have allowed a better feedforward transmission of information during task performance. During the behavioral task used in this work, a decreased activity of PV+ neurons could improve the transmission of both stimulus types to allow a better discrimination. This hypothesis remains to be tested.

In general, the distinct roles of all interneuron subtypes in cortical activity are diverse. Several studies have investigated the contribution of different interneuron subtypes to stimulus selectivity and showed that PV+ and SOM+ have different roles in the tuning of excitatory neurons (e.g. Atallah et al., 2012; El-Boustani and Sur, 2014; Lee et al., 2012; Wilson et al., 2012). However, the results of these studies on the specific role of each interneuron subtype are controversial. Some

studies found that SOM+ neurons sharpen orientation tuning (Wilson et al., 2012), while PV+ activation showed only small effects on tuning but changed response gain (Atallah et al., 2012; El-Boustani and Sur, 2014; Wilson et al., 2012). Other studies showed that PV+, but not SOM+ neuron activity sharpens tuning (Lee et al., 2012). In follow-up studies the authors recognized that most of the disagreement was due to the protocols used to stimulate the interneurons (Lee et al., 2014). This implies that the function of different interneuron subtypes is not a fixed property but rather a dynamic function that depends on visual stimulation, brain state or context. Therefore, how these different subtypes of interneurons might influence response properties to behaviorally-relevant stimuli is not well understood.

The activity of putative interneurons in this work is mostly represented by PV+ neurons. The results indicate that this subgroup of interneurons shows very similar activity in comparison to pyramidal cells and might well be implicated in task dependent changes in firing rates of the V1 population. The group of putative inhibitory interneurons and even the subgroup of tagged PV+ neurons is likely to contain further distinct subgroups (Markram et al., 2004) which could show different activity patterns during different conditions. In future experiments it might be important to refine the definition of inhibitory interneurons and record from larger ensembles of different subtypes at the same time and during different behaviors.

5 Conclusion

In this work I have presented a new behavioral paradigm to assess task dependent changes in sensory processing of mice. The stimuli used in this paradigm provided the same sensory drive to recorded neurons and at the same time allowed manipulation of behavioral relevance by different reward assignments to the stimuli. By comparing the neural representation of the stimuli during phases of task engagement and passive viewing, I found, in the primary visual cortex of the mouse, a substantial number of neurons, whose responses were modulated by behavioral context. In comparison, a smaller fraction of dLGN neurons showed such modulation, suggesting an amplification of effects along the visual processing hierarchy as is the case in primates. Since running speed and eye positions were matched during a critical time window, these task-dependent modulations presumably originate from an internal, nonsensory source. These results are remarkable, since they offer new insights for future investigations of how top-down modulations might shape sensory processing to enhance the neural representation of behaviorally relevant information. In further investigations, optogenetic techniques might help to explore certain cell types or neural circuits and their role in top-down modulation to establish the neural basis of visual behavior. Taken together, this work shows that the mouse is a useful model to study how the visual system transforms sensory signals into task-related representations.

6 Materials and Methods

I used 19 mice (3-4 months old, 11 males and 8 females), 9 of the C57BL/6J wild type strain and 10 of the PV-Cre strain B6;129P2-Pvalbtm1(cre)Arbr/J (JAX stock number 008069). All procedures were carried out in compliance with the European Communities Council Directive 2010/63/EC and the German Law for Protection of Animals; they were approved by the local authorities following appropriate ethics review.

6.1 Surgical protocol

Anesthesia was induced with Isoflurane (3 %) and maintained throughout the surgery (1.5%). A small L-shaped aluminum head post was attached to the anterior part of the skull (OptiBond FL primer and adhesive, Kerr dental; Tetric EvoFlow dental cement, Ivoclar vivadent); two miniature screws (00-96 x 1/16 stainless steel screws, Bilaney) were implanted over the cerebellum serving as reference and ground for electrophysiological recordings. Before surgery, an analgesic (Buprenorphine, 0.1 mg/kg sc) was administered, and the eyes were protected with ointment (Bepanthen). The animal's temperature was kept at 37 C° via a feedback controlled heating pad (WPI). Antibiotics (Baytril, 5 mg/kg sc) and a longer lasting analgesic (Carprofen, 5 mg/kg sc) were administered for 3 days post-surgery. Expression of channelrhodopsin (ChR2) in PV-Cre mice was achieved by injecting into V1 of anesthetized animals, through a small craniotomy, the adeno-associated viral vector rAAV5.EF1a.DIO.hChR2(H134R)-EYFP.WPRE.hGH (Penn Vector Core, University of Pennsylvania). A Picospritzer III (Parker) was used to inject the virus at multiple depths while gradually retracting the pipette. Mice were given 7 days to recover before they were habituated to the experimental setup. Before electrophysiological recordings, a craniotomy ($\sim$ 1.5 mm^2) was performed over V1 (3 mm lateral to the midline and 1.1 mm anterior to the transverse sinus (Wang et al., 2011) or over the dorsal part of the lateral geniculate nucleus (dLGN, 2.3 mm lateral to the midline and 2 mm anterior of lambda suture (Piscopo et al., 2013)) or over the anterior cingulate cortex (0.2 anterior to bregma and 0.3 mm lateral from midline (Zhang et al., 2014)). The craniotomy was sealed with Kwik-Cast (WPI), which was removed and re-applied before and after each recording session.

6.2 Experimental procedure

6.2.1 Experimental Setup

Mice were put on an air-cushioned Styrofoam ball (n = 11) or a mounted plastic disk (n = 8) and head-fixed by clamping their head-post to a rod. Movements of the ball were recorded at 90 Hz by two optical mice connected to a microcontroller (Arduino Duemilanove); disk rotation was measured with a rotary encoder sampling at 100 Hz (MA3-A10-125-N Magnetic Encoder, Pewatron). A computer-controlled syringe pump (Aladdin AL-1000, WPI) delivered precise amounts of water through a drinking spout, which was positioned in front of the animals' snout. The drinking spout was present only during the foraging task experiments and was removed during measurements in passive viewing conditions. Visual stimuli were generated with custom-written software (https://sites.google.com/a/nyu.edu/expo/home) and presented on a liquid crystal display (LCD) monitor 25 cm in front of the animals' eyes (Samsung 2233RZ, mean luminance of 50 cd/m^2, refresh rate 120 Hz). Luminance non-linearities of the display were corrected with an inverse gamma lookup table, which was regularly obtained by calibration with a photometer. Stimuli consisted of sinusoidal gratings, which were 40-55 deg in diameter, and were framed by either a black square or diamond. In a separate block of trials, the same stimuli were presented in a passive viewing conditions. The duration of the stimulus was 2s and the intertrial interval was 0.5 s. During these trials the drinking spout was removed and stimulus presentation was unrelated to the animals' running behavior. Due to an error in the program generating the stimuli, the phase of the drifting grating in passive viewing experiments was shifted by 270° relative to the phase of the grating in task experiments. The position of the stimuli was chosen to overlap with as many RFs as possible. Temporal frequency was 1.5 Hz for recordings from V1, or 4 Hz for recordings from dLGN, spatial frequency was 0.02-0.05 cycles/deg, the drift direction was 0 deg. Orientation tuning was measured by presenting sinusoidal gratings moving in a randomly selected direction (12 levels) for a duration of 2 s. Intertrial interval was 0.5 s. A blank screen condition (mean luminance) was included to estimate spontaneous firing rate. The setup was enclosed within a black fabrics curtain. Eye movements were monitored under infrared illumination using a zoom lens (Navitar Zoom 6000) coupled to a camera (Guppy AVT, frame rate 50 Hz).

6.2.2 Initial behavioral training

After recovering from the surgery for one week, animals were placed on a water restriction schedule until their weight dropped to ~ 85 % of their ad libitum body weight. During this time, mice were habituated to head-fixation on the ball or disk and delivery of water through the spout. The animals' weight and fluid consumption were monitored and recorded on each day, and the animals were checked for potential signs of dehydration. After the weight had stabilized the visual foraging task sessions started. These were typically performed 5 days a week, and only during these sessions mice received water.

6.2.3 Visual foraging task

Animals were trained to discriminate between 2 stimuli, a downward moving drifting grating either behind a diamond or a square aperture. Mice could control the appearance of the stimuli with their running speed on the treadmill. To start a trial, mice needed, after stopping for a short time, to cross a speed threshold of 5 cm/s for the time of 500 ms. After trial initiation one of the two stimuli appeared on the monitor with one stimulus signaling the presence of an upcoming reward ('go' stimulus) and the other signaling the absence of a reward ('stop' stimulus). During the go-stimulus presentation, mice could earn a reward by running for an additional 4 s (6-9 µl). If the animal responded with a 4-s run to the go-stimulus, it was considered a hit trial. Otherwise, if the mouse was running 4 s in response to the stop-stimulus, there were no consequences and the response was considered a false alarm. Additionally, at any point in time mice could reject a trial by immediately slowing down again. In that case the stimulus disappeared, and the mouse could immediately start a new trial again, which would save energy and time to get to a new trial. Terminated trials were considered correct aborts if the stop-stimulus was shown and incorrect aborts if the go-stimulus was shown. A single session consisted of 300 – 600 trials per day, divided into blocks of 100 trials.

6.2.4 Electrophysiological recordings

After animals have learned the visual task, extracellular recordings were performed with 32-channel linear silicon probes (Neuronexus, A1x32-5mm-25-177-A32 for V1 and ACC recordings, A1x32-5mm-25-177-Edge for LGN recordings). Electrodes were inserted perpendicular to the brain surface and lowered to ~800 µm (V1) or ~2500 µm (LGN) or ~1100 µm (ACC) below the surface. Wideband extracellular signals were digitized at 30 kHz (Blackrock microsystems) and analyzed using the NDManager software suite. To isolate single

neurons from linear arrays, I grouped adjacent channels into 5 equally sized "virtual octrodes" (8 channels per group with 2 channels overlap). Using an automatic spike detection threshold (Quiroga et al., 2004), spikes were extracted from the high-pass filtered continuous signal for each group separately. The first 3 principal components of each channel were used for automatic clustering with KlustaKwik (K. D. Harris, http://klusta-team.github.io/klustakwik), which was followed by manual refinement of clusters (Hazan et al., 2006). In the analyses of neural data, I only considered high-quality single unit activity, judged by the distinctiveness of the spike wave shape and cleanness of the refractory period in the autocorrelogram.

6.2.5 Optogenetic tagging

For identification of V1 PV+ inhibitory interneurons in our extracellular recordings, I performed optogenetic tagging experiments 3-4 weeks after virus injection. I used a fiber-coupled light-emitting diode (LEDs, Doric lenses) with a wavelength of 470 nm, driven by a LED driver (LEDD1B, Thorlabs). The fiber was 1 mm^2 in diameter and the LED light intensity, measured at the tip of the fiber, was 2.6-3.5 mW/mm^2. The optic fiber was lowered with a micromanipulator to less than 1 mm over the exposed V1; I aimed at the most perpendicular positioning of the fiber with respect to the brain surface, to avoid potential photoelectric interferences with recorded neural activity at light onsets (see (Cardin et al., 2010)). The animal's eyes were shielded from the blue light by a sheet of black non-reflecting aluminum foil placed around the stimulation site.

For optogenetic tagging, I followed the protocol described by (Kvitsiani et al., 2013); I delivered bursts of 10 x 1ms light pulses at 10 Hz during spontaneous activity, or a 1ms pulse at half ISI during an orientation tuning experiment.

6.2.6 Identification of V1 PV+ inhibitory interneurons with opto-tagging

I identified PV+ interneurons in the extracellular recordings based on an adjusted version of the SALT test (stimulus-associated spike latency test) (Kvitsiani et al., 2013). Briefly, I compared the distribution of first spike latencies in a 10ms window after a 1ms optogenetic light stimulation to control distributions obtained from baseline periods without light stimulation. Neurons were considered tagged if the information distance between the distributions was greater than 0.08 and statistically different at a significance level of $p < 0.01$. In addition, I requested that prolonged optogenetic stimulation yielded at least 8-fold, reliable ($p < 10^{-5}$) increases of firing rates.

6.3 Analysis of behavior

6.3.1 Behavioral performance

I quantified behavioral task performance for each recording session with a behavioral dprime. Hit and false alarm rates were quantified as follows:

Hit rate = number of hits / (number of hits + number of incorrect aborts)
False alarm (FA) rate = number of FAs / (number of FAs + number of correct aborts)

With hit and false alarm rates I then quantified d' as follows:

d' = norminv(hit rate) – norminv(FA rate), where norminv is the inverse of the cumulative normal function. Higher d' values indicate better performance, I considered mice being trained when d' > 1.5.

Behavioral d' can be infinite, if the animal shows perfect behavior and the hit rate results in 1, or the false alarm rate results in 0. To avoid infinite d' values, perfect behavior was corrected as follows (Stanislaw and Todorov, 1999):

Hit rate = number of hits + 0.5 / (number of hits + number of incorrect aborts + 1)
False alarm (FA) rate = number of FAs + 0.5 / (number of FAs + number of correct aborts + 1)

6.3.2 Running behavior

I recorded ball movements during all sessions, by means of two optical mice placed at the sides of the spherical treadmill. I used the Euclidean norm of three perpendicular components of ball velocity (roll, pitch and yaw) to compute the animals' running speed.

When animals were trained, running speed changed quickly after stimulus onset. To identify invalid trials, first I applied some exclusion criteria. I removed trials in which trial termination happened too fast (0 – 500 ms after trial onset) or too slow (2 s after trial onset). Furthermore, I excluded trials in every series which were lower than 2-5 times the standard error of the mean speed of correct abort trials. To determine the time point of speed divergence, I separated single-trial speed profiles into 2 groups according to the trial outcome hit or correct abort. Then I performed, to obtain the time window of same running speed between task

conditions, across the distributions of hit and correct abort trials, for every point in time a nonparametric Kolmogorov-Smirnov test and determined the first point of three consecutive significant values ($p < 0.01$) as time point of speed divergence.

6.3.3 Eye position

The pupil detection in our eye tracking data was performed with a custom-written program developed with the Bonsai framework (Lopes et al., 2015). Briefly, I applied a threshold to turn each camera frame into a binary image, performed a morphological opening operation, identified the most circle-like object as the pupil, and fitted a circle to determine the position of its center. I computed relative pupil displacements by subtracting, for each frame, the pupil position from a default position, defined as the grand average eye position across all stimuli and task conditions. To convert pupil displacements to angular displacements, I assumed that the center of eye rotation was 1.041 mm behind the pupil (Stahl et al., 2000). I defined saccades as changes in eye position > 2 deg. Considering that the average mouse saccade lasts 50 ms (Sakatani and Isa, 2007), I detected saccades by taking the difference of mean eye position 60 ms before and after each time point. Differences in saccade frequencies across all four stimulus conditions (square and diamond during task and passive viewing) were assessed by performing a 2x2 ANOVA on percentages of saccade trials involving the within-subject factors task condition (task vs. passive viewing) and stimulus (go vs. stop stimulus).

To correct for different eye positions in task as well as control conditions, I carefully matched eye positions in following procedure: (1) For each trial, I aligned eye positions to stimulus onset. I extracted eye positions in a time window where running speed was indistinguishable and, in this window, removed saccade trials. Within this time window I computed, for every trial, the mean eye position across time. To compare the distributions of eye positions across all 4 conditions without binning, I used the multisample variant of the nonparametric Anderson–Darling test (Scholz and Stephens, 1987). This is an omnibus test and provides a single test statistic to assess whether multiple distributions differ from each other. (2) Because the eye position distributions differed from each other in every single recording session (see **Figure 9**, left), I applied a stratification procedure to match eye positions. Eye positions from task and control experiments within a series were compiled, sorted into bins of 1-7 deg, into a 2-D histogram, separate for vertical and horizontal eye positions. (3) Eye positions of four conditions were matched by matching the counts of eye positions within bins across the two control stimuli and the two task stimuli (see **Figure 8**E-F for example). Eye positions across all 4 conditions were considered matched, if the Anderson-Darling

test of eye position distribution in each horizontal and vertical plane revealed a p-value > 0.1 (see **Figure 8**G-H, for example).

6.4 Analysis of neural data

6.4.1 Measurement of response properties

Before each behavioral task experiment, I mapped RF properties. RFs were mapped with a sparse noise stimulus, consisting of 5 degree full-contrast black and white squares, which were flashed individually, on a gray background, for 150ms at a random location in a virtual 12 x 12 grid. Responses were fitted with a 2D ellipse to determine RF center, separately for ON and OFF subfields (Liu et al., 2010).

6.4.2 Neural discriminability

Recordings were only performed on trained mice, which showed a stable task performance over at least two days. For the analyses of neural data, I only included data which were obtained during experiments with good behavioral performance (d' > 1.5). Additionally, only recording sessions were included, in which eye position matching could be accomplished successfully. Spike density functions (see **Figure 10**A,C) were computed by convolving spike-trains of the whole experiment with a Gaussian kernel (kernel resolution 10ms), then cut into individual trials and averaged across them. In the analysis of neural discriminability, I included neurons if their mean firing rate was, in a separate orientation tuning experiment, at least 1 spike/s across stimulus orientations.

I quantified how well individual neurons can discriminate between the go and stop stimulus by extracting single-trial mean firing rates in time windows from 0 s to the time point of speed divergence after stimulus onset. Through the stratification procedure, where I matched eye positions across stimulus conditions, I selected a random subset of trials. For each experiment condition, task and passive viewing, strengths of discriminability between the two stimuli were quantified by calculating the area under the receiver operating characteristic (ROC) curve based on single trial responses. The ROC curve is a nonparametric measure of the discriminability of two distributions. ROC values of 0.5 indicate that an ideal observer can only perform at chance level in discriminating between the two stimuli. Higher or lower ROC values indicate stronger responses to one of the two stimuli. I repeated these steps 1000 times to construct a distribution of ROC values. Because in the passive viewing experiments, the stimulus phase of the drifting

grating was shifted by 270°, I performed the same analysis again, by shifting the time window in the passive viewing condition, such that the phases of the gratings during passive viewing and task were identical. In the tuning experiment, a single unit is marked as significant if the chance-level ROC value (0.5) is outside the central 99% of the distribution of all ROC values. It's enough if the value is outside for one combination of time windows, be it the time window from stimulus onset to the point of speed divergence or the correspondent time window with matched phases. In the task experiment, a unit was considered significant if chance level was outside the 99% for both combinations of time windows. To make sure that identical sensory stimulation was provided to neurons, I only included neurons in my analyses, which could not discriminate between the go and stop stimulus during passive viewing in both time windows. In rare cases, non-significant AUC values in the passive viewing condition deviate stronger from chance level, and therefore show a stronger effect, than significant AUC values during passive viewing (see e.g. highest data point during passive viewing in **Figure 11**). This is due to a high variability and a broad distribution of ROC values with the chance-level ROC value (0.5) within the central 99% of the distribution of all ROC values in one case, but not the other. The same procedure was done in either dataset, either obtained from V1 or dLGN.

6.5 Histology

For histological analysis, mice were transcardially perfused under deep anesthesia first with 0.2 M sodium phosphate buffer (PBS), followed by 4% paraformaldehyde in PBS. Brains were postfixed for 24 hours at 4° and then stored in PBS. Coronal sections (40 μm) were cut using a vibratome (Microm HM 650 V-Thermo Scientific) and mounted on glass slides with Vectashield DAPI (Vector Laboratories). Slices were inspected with a Zeiss Imager.Z1m fluorescent microscope. For optogenetic tagging experiments, viral expression was confirmed by the presence of YFP-labeled PV+ interneurons across the V1 cortical thickness. For targeted dLGN recordings, electrodes were coated before insertion into the brain with a magenta-shifted fluorescent liphophilic tracer (DiD; D7757, Invitrogen). Mice underwent perfusion as described above, and brain slices were subsequently inspected for the presence of DiD trace reaching dLGN.

7 Acknowledgements

I am very thankful to Dr. Steffen Katzner for his great supervision and the opportunity to complete this work in his lab. Especially I want to thank him for giving me the opportunity to get international experience and present my data on international conferences and a summer school. Also, I want to thank Prof. Dr. Laura Busse for many scientific discussions and feedback regarding my results. I want to thank Prof. Dr. Joachim Ostwald and Prof. Dr. Ziad Hafed for being in my advisory board committee and giving me supportive feedback throughout the years.

Further I want to thank all my lab mates for many years of successful, peaceful and fun cooperation. Dr. Ovidiu Jurjut I want to thank for being a loyal sitting neighbor and supporting me in developing my programming skills. I want to thank Dr. Agne Klein for a successful collaboration and providing dLGN data, Dr. Petya Georgieva for supporting me with training my animals and doing recordings and Matilde Fiorini, Sinem Erisken, Miroslav Roman-Roson and Dr. Zeinab Khastkhodaei for helping with all the other small things in the daily lab business. My two master students, Frederike Klein and Gregory Born, I want to thank just for being nice and motivated master students and helping me with my project.

Finally, I want to thank my family and friends for always being there and supporting me, even though they would not really understand what I was doing over all the years. Thanks to my family for all the great food and more, and to my friends for fun weekends and great holidays. I am also thankful for many rides through beautiful landscapes with members of the RV Pfeil Tübingen. Last, I want to thank Peter for all the support during the last years, beautiful bike rides and especially for introducing pumpkin pie to me.

8 References

Andermann, M.L. (2010). Chronic cellular imaging of mouse visual cortex during operant behavior and passive viewing. Front. Cellullar Neurosci. *4*, 1–16.

Andermann, M.L., Kerlin, A.M., and Reid, R.C. (2010). Chronic cellular imaging of mouse visual cortex during operant behavior and passive viewing. Front. Cellullar Neurosci. *4*, 1–16.

Andermann, M.L., Kerlin, A.M., Roumis, D.K., Glickfeld, L.L., and Reid, R.C. (2011). Functional specialization of mouse higher visual cortical areas. Neuron *72*, 1025–1039.

Anzai, A., Peng, X., and Van Essen, D.C. (2007). Neurons in monkey visual area V2 encode combinations of orientations. Nat. Neurosci. *10*, 1313–1321.

Atallah, B. V., Bruns, W., Carandini, M., and Scanziani, M. (2012). Parvalbumin-Expressing Interneurons Linearly Transform Cortical Responses to Visual Stimuli. Neuron *73*, 159–170.

Ayaz, A., Saleem, A.B., Schölvinck, M.L., and Carandini, M. (2013). Locomotion controls spatial integration in mouse visual cortex. Curr. Biol. *23*, 890–894.

Baluch, F., and Itti, L. (2011). Mechanisms of top-down attention. Trends Neurosci. *34*, 210–224.

Van Den Bergh, G., Zhang, B., Arckens, L., and Chino, Y.M. (2010). Receptive-field properties of V1 and V2 neurons in mice and macaque monkeys. J. Comp. Neurol. *518*, 2051–2070.

Bisley, J.W., and Goldberg, M.E. (2003). Neuronal activity in the lateral intraparietal area and spatial attention. Science (80-.). *299*, 81–86.

Bonin, V., Histed, M.H., Yurgenson, S., and Reid, R.C. (2011). Local diversity and fine-scale organization of receptive fields in mouse visual cortex. J. Neurosci. *31*, 18506–18521.

Bortone, D.S., Olsen, S.R., and Scanziani, M. (2014). Translaminar inhibitory cells recruited by layer 6 corticothalamic neurons suppress visual cortex. Neuron *82*, 474–485.

Buffalo, E.A., Fries, P., Landman, R., Liang, H., and Desimone, R. (2010). A backward progression of attentional effects in the ventral stream. Proc. Natl. Acad. Sci. U. S. A. *107*, 361–365.

Burgess, C.P., Steinmetz, N.A., Lak, A., Zatka-Haas, P., Ranson, A., Wells, M.J., Schroeder, S., Jacobs, E.A.K.K., Bai Reddy, C., Soares, S., et al. (2017). High-yield methods for accurate two-alternative visual psychophysics in head-fixed mice. bioRxiv *20*, 51912.

Busse, L., Katzner, S., Tillmann, C., and Treue, S. (2008). Effects of attention on perceptual direction tuning curves in the human visual system. J. Vis. *8*, 2–2.

Busse, L., Ayaz, A., Dhruv, N.T., Katzner, S., Saleem, A.B., Scholvinck, M.L., Zaharia, A.D., and Carandini, M. (2011). The Detection of Visual Contrast in the Behaving Mouse. J. Neurosci. *31*, 11351–11361.

Callaway, E.M. (1998). Local Circuits in Primary Visual Cortex of the Macaque Monkey. Annu. Rev. Neurosci. *21*, 47–74.

Callaway, E.M. (2004). Feedforward, feedback and inhibitory connections in primate visual cortex. Neural Networks *17*, 625–632.

Carandini, M., and Churchland, A.K. (2013). Probing perceptual decisions in rodents. Nat. Neurosci. *16*, 824–831.

Cardin, J.A., Carlén, M., Meletis, K., Knoblich, U., Zhang, F., Deisseroth, K., Tsai, L.-H., and Moore, C.I. (2010). Targeted optogenetic stimulation and recording of neurons in vivo using cell-type-specific expression of Channelrhodopsin-2. Nat. Protoc. *5*, 247–254.

Carrasco, M. (2011). Visual attention: The past 25 years. Vision Res. *51*, 1484–1525.

Chelazzi, L., Duncan, J., Miller, E.K., and Desimone, R. (1998). Responses of Neurons in Inferior Temporal Cortex During Memory- Guided Visual Search. J. Neurophysiol. *80*, 2918–2940.

Chen, C., Ignashchenkova, A., Thier, P., Hafed, Z.M., Chen, C., Ignashchenkova, A., Thier, P., and Hafed, Z.M. (2015). Neuronal Response Gain Enhancement prior to Article Neuronal Response Gain Enhancement prior to Microsaccades. Curr. Biol. *25*, 2065–2074.

Chen, Y., Martinez-Conde, S., Macknik, S.L., Bereshpolova, Y., Swadlow, H.A., and Alonso, J.-M.M. (2008). Task difficulty modulates the activity of specific neuronal populations in primary visual cortex. Nat. Neurosci. *11*, 974–982.

Chubykin, A.A., Roach, E.B., Bear, M.F., and Shuler, M.G.H. (2013). A Cholinergic Mechanism for Reward Timing within Primary Visual Cortex. Neuron *77*, 723–735.

Cossell, L., Iacaruso, M.F., Muir, D.R., Houlton, R., Sader, E.N., Ko, H., Hofer, S.B., and Mrsic-flogel, T.D. (2015). Functional organisation of excitatory synaptic strength in primary visual cortex. Nature.

Deisseroth, K. (2015). Optogenetics: 10 years of microbial opsins in neuroscience. Nat. Neurosci. *18*, 1213–1225.

Desimone, R., Albright, T.D., Gross, C.G., and Bruce, C. (1984). Stimulus-selective properties of inferior temporal neurons in the macaque. J. Neurosci. *4*, 2051–2062.

Drager, U.C. (1975). Receptive fields of single cells and topography in mouse visual cortex. J. Comp. Neurol. *160*, 269–290.

El-Boustani, S., and Sur, M. (2014). Response-dependent dynamics of cell-specific inhibition in cortical networks in vivo. Nat. Commun. *5*, 5689.

Erisken, S., Vaiceliunaite, A., Jurjut, O., Fiorini, M., Katzner, S., and Busse, L. (2014). Effects of Locomotion Extend throughout the Mouse Early Visual System. Curr. Biol. *24*, 1–9.

Felleman, D.J., and Van Essen, D.C. (1991). Distributed hierarchical processing in the primate cerebral cortex. Cereb. Cortex *1*, 1—47.

Freeman, J., Ziemba, C.M., Heeger, D.J., Simoncelli, E.P., and Movshon, J.A. (2013). A functional and perceptual signature of the second visual area in primates. Nat. Neurosci. *16*, 974–981.

Fu, Y., Tucciarone, J.M., Espinosa, J.S., Sheng, N., Darcy, D.P., Nicoll, R.A., Huang, Z.J., and Stryker, M.P. (2014). A Cortical Circuit for Gain Control by Behavioral State. Cell *156*, 1139–1152.

Gao, E., DeAngelis, G.C., and Burkhalter, A. (2010). Parallel Input Channels to Mouse Primary Visual Cortex. J. Neurosci. *30*, 5912–5926.

Gilbert, C.D., and Li, W. (2013). Top-down influences on visual processing. Nat. Rev. Neurosci. *14*, 350–363.

Glickfeld, L.L., Andermann, M.L., Bonin, V., and Reid, R.C. (2013a). Cortico-cortical projections in mouse visual cortex are functionally target specific. Nat. Neurosci. *16*, 219–226.

Glickfeld, L.L., Histed, M.H., and Maunsell, J.H.R. (2013b). Mouse Primary Visual Cortex Is Used to Detect Both Orientation and Contrast Changes. J. Neurosci. *33*, 19416–19422.

Glimcher, P.W. (2003). The neurobiology of visual-saccadic decision making. Annu. Rev. Neurosci. *26*, 133–179.

Gold, J.I., and Shadlen, M.N. (2007). The Neural Basis of Decision Making. Annu. Rev. Neurosci. *30*, 535–574.

Gonchar, Y., and Burkhalter, A. (1997). Three distinct families of GABAergic neurons in rat visual cortex. Cereb. Cortex *7*, 347–358.

Grubb, M.S. (2003). Quantitative Characterization of Visual Response Properties in the Mouse Dorsal Lateral Geniculate Nucleus. J. Neurophysiol. *90*, 3594–3607.

Guo, Z., Li, N., Huber, D., Ophir, E., and Gutnisky, D. (2014). Flow of Cortical Activity Underlying a Tactile Decision in Mice. Neuron *81*, 179–194.

Hafed, Z.M., and Clark, J.J. (2002). Microsaccades as an overt measure of covert attention shifts. Vision Res. *42*, 2533–2545.

Hafed, Z.M., Lovejoy, L.P., and Krauzlis, R.J. (2011). Modulation of Microsaccades in Monkey during a Covert Visual Attention Task. J. Neurosci. *31*, 15219–15230.

Hamilton, L.S., Sohl-Dickstein, J., Huth, A.G., Carels, V.M., Deisseroth, K., and Bao, S. (2013). Optogenetic Activation of an Inhibitory Network Enhances Feedforward Functional Connectivity in Auditory Cortex. Neuron *80*, 1066–1076.

Hazan, L., Zugaro, M., and Buzsáki, G. (2006). Klusters, NeuroScope, NDManager: A free software suite for neurophysiological data processing and visualization. J. Neurosci. Methods *155*, 207–216.

Herrero, J.L., Roberts, M.J., Delicato, L.S., Gieselmann, M.A., Dayan, P., and Thiele, A. (2008). Acetylcholine contributes through muscarinic receptors to attentional modulation in V1. Nature *454*, 1110–1114.

Histed, M.H., Carvalho, L.A., and Maunsell, J.H.R. (2012). Psychophysical measurement of contrast sensitivity in the behaving mouse. J. Neurophysiol. *107*, 758–765.

Hofer, S.B., Ko, H., Pichler, B., Vogelstein, J., Ros, H., Zeng, H., Lein, E., Lesica, N.A., and Mrsic-Flogel, T.D. (2011). Differential connectivity and response dynamics of excitatory and inhibitory neurons in visual cortex. Nat. Neurosci. *14*, 1045–1052.

Hubel, D.H., and Wiesel, T.N. (1959). Receptive fields of single neurones in the cat's striate cortex. J. Neurophysiol. *148*, 574–591.

Hubel, D.H., and Wiesel, T.N. (1977). Functional architecture of macaque monkey visual cortex. Proc. R. Soc. Lond. *198*, 1–59.

Hübener, M. (2003). Mouse visual cortex. Curr. Opin. Neurobiol. *13*, 413–420.

Huberman, A.D., and Niell, C.M. (2011). What can mice tell us about how vision works? Trends Neurosci. *34*, 464–473.

Hut, R.A., Pilorz, V., Boerema, A.S., Strijkstra, A.M., and Daan, S. (2011). Working for food shifts nocturnal mouse activity into the day. PLoS One *6*, 1–6.

Isaacson, J.S., and Scanziani, M. (2011). How inhibition shapes cortical activity. Neuron *72*, 231–243.

Ito, M., and Gilbert, C. (1999). Attention modulates contextual influence in the Primary Visual Cortex of Alert Monkeys. Neuron *22*, 593–604.

Jaramillo, S., and Zador, A.M. (2011). The auditory cortex mediates the perceptual effects of acoustic temporal expectation. Nat. Neurosci. *14*, 246–251.

Jeon, C.J., Strettoi, E., and Masland, R.H. (1998). The major cell populations of the mouse retina. J. Neurosci. *18*, 8936–8946.

Jurjut, O., Georgieva, P., Busse, L., and Katzner, S. (2017). Learning enhances sensory processing in mouse V1 before improving behavior. J. Neurosci. *37*, 1–29.

Karnani, M.M., Agetsuma, M., and Yuste, R. (2014). A blanket of inhibition: Functional inferences from dense inhibitory connectivity. Curr. Opin. Neurobiol. *26*, 96–102.

Karnani, M.M., Jackson, J., Ayzenshtat, I., Tucciarone, J., Manoocheri, K., Snider, W.G., Yuste, R., Bathellier, B., Ushakova, L., Rumpel, S., et al. (2016). Cooperative Subnetworks of Molecularly Similar Interneurons in Mouse Neocortex. Neuron *90*, 86–100.

Katzner, S., and Weigelt, S. (2013). Visual cortical networks: Of mice and men. Curr Opin Neurobiol *23*, 202–206.

Katzner, S., Busse, L., and Carandini, M. (2011). GABAA Inhibition Controls Response Gain in Visual Cortex. J. Neurosci. *31*, 5931–5941.

Kawai, R., Markman, T., Poddar, R., Ko, R., Fantana, A.L., Dhawale, A.K., Kampff, A.R., and Ölveczky, B.P. (2015). Motor Cortex Is Required for Learning but Not for Executing a Motor Skill. Neuron *86*, 800–812.

Keller, G.B., Bonhoeffer, T., and Hübener, M. (2012). Sensorimotor Mismatch Signals in Primary Visual Cortex of the Behaving Mouse. Neuron *74*, 809–815.

Khastkhodaei, Z., Jurjut, O., Katzner, S., and Busse, L. (2016). Mice Can Use Second-Order, Contrast-Modulated Stimuli to Guide Visual Perception. J. Neurosci. *36*, 4457–4469.

Kvitsiani, D., Ranade, S., Hangya, B., Taniguchi, H., Huang, J.Z., and Kepecs, a (2013). Distinct behavioural and network correlates of two interneuron types in prefrontal cortex. Nature *498*, 363–366.

Lamme, V. a F., Supèr, H., and Spekreijse, H. (1998). cortex and feedback processing in the visual Hans Sup & and Henk Spekreijse. Curr. Opin. Neurobiol. *8*, 529–535.

Lee, S.-H., Kwan, A.C., Zhang, S., Phoumthipphavong, V., Flannery, J.G., Masmanidis, S.C., Taniguchi, H., Huang, Z.J., Zhang, F., Boyden, E.S., et al. (2012). Activation of specific interneurons improves V1 feature selectivity and visual perception. Nature *488*, 379–383.

Lee, S.-H., Kwan, A.C., and Dan, Y. (2014). Interneuron subtypes and orientation tuning. Nature *508*, E1–E2.

Leopold, D.A., and Logothetis, N.K. (1998). Microsaccades differentially modulate neural activity in the striate and extrastriate visual cortex. Exp. Brain Res. *123*, 341–345.

Lien, A.D., and Scanziani, M. (2013). Tuned thalamic excitation is amplified by visual cortical circuits. Nat. Neurosci. *16*, 1315–1323.

Liu, B., Li, P., Sun, Y.J., Li, Y., Zhang, L.I., and Tao, H.W. (2010). Intervening inhibition underlies simple-cell receptive field structure in visual cortex. Nat. Neurosci. *13*, 89–96.

Loftus, G.R., and Masson, M.E.J. (1994). Using confidence intervals in within-subject designs. Psychon. Bull. Rev. *1*, 476–490.

Lopes, G., Bonacchi, N., Frazao, J., Neto, J.P., Atallah, B. V., Soares, S., Moreira, L., Matias, S., Itskov, P.M., Correia, P.A., et al. (2015). Bonsai: an event-based framework for processing and controlling data streams. Front. Neuroinform. *9*, 1–14.

Luck, S.J., Chelazzi, L., Hillyard, S.A., and Desimone, R. (1997). Neural mechanisms of spatial selective attention in areas V1, V2, and V4 of macaque visual cortex. J. Neurophysiol. *77*, 24–42.

Macmillan, N.A., and Creelman, C.D. (1991). Detection theory: A user's guide. (New York, NY, US: Cambridge University Press).

Maimon, G. (2011). Modulation of visual physiology by behavioral state in monkeys, mice, and flies. Curr. Opin. Neurobiol. *21*, 559–564.

Makino, H., and Komiyama, T. (2015). Learning enhances the relative impact of top-down processing in the visual cortex. Nat. Neurosci. *2015*.

Marbach, F., and Zador, A.M. (2016). A self-initiated two-alternative forced choice paradigm for head-fixed mice. bioRxiv 73783.

Markram, H., Toledo-Rodriguez, M., Wang, Y., Gupta, A., Silberberg, G., and Wu, C. (2004). Interneurons of the neocortical inhibitory system. Nat. Rev. Neurosci. *5*, 793–807.

Marshel, J.H., Garrett, M.E., Nauhaus, I., and Callaway, E.M. (2011). Functional specialization of seven mouse visual cortical areas. Neuron *72*, 1040–1054.

Marshel, J.H., Kaye, A.P., Nauhaus, I., and Callaway, E.M. (2012). Anterior-Posterior Direction Opponency in the Superficial Mouse Lateral Geniculate Nucleus. Neuron *76*, 713–720.

Maunsell, J.H.R. (2015). Neuronal Mechanisms of Visual Attention. Annu. Rev. Vis. Sci. *1*, 373–391.

Maunsell, J.H.R., and Cook, E.P. (2002). The role of attention in visual processing. Philos. Trans. R. Soc. B Biol. Sci. *357*, 1063–1072.

Mayrhofer, J.M., Skreb, V., von der Behrens, W., Musall, S., Weber, B., and Haiss, F. (2013). Novel two-alternative forced choice paradigm for bilateral vibrotactile whisker frequency discrimination in head-fixed mice and rats. J. Neurophysiol. *109*, 273–284.

McAdams, C.J., and Maunsell, J.H.R. (1999). Effects of Attention on the Reliability of Individual Neurons in Monkey Visual Cortex. Neuron *23*, 765–773.

McAlonan, K., Cavanaugh, J., and Wurtz, R.H. (2008). Guarding the gateway to cortex with attention in visual thalamus. Nature *456*, 391–394.

Métin, C., Godement, P., and Imbert, M. (1988). The primary visual cortex in the mouse: receptive field properties and functional organization. Exp. Brain Res. *69*, 594–612.

Miller, E.K., and Cohen, J.D. (2001). An integrative theory of prefrontal cortex function. Annu. Rev. Neurosci. 167–202.

Mitchell, J.F., Sundberg, K.A., and Reynolds, J.H. (2007). Differential attention-dependent response modulation across cell classes in macaque visual area V4. Neuron *55*, 131–141.

Moore, T. (2001). Control of eye movements and spatial attention. Proc. Natl. Acad. Sci. *98*, 1273–1276.

Moore, T., and Armstrong, K.M. (2003). Selective gating of visual signals by microstimulation of frontal cortex. Nature *421*, 370–373.

Moran, J., and Desimone, R. (1985). Selective attention gates visual processing in the extrastriate cortex. Science (80-.). *229*, 782–784.

Motter, B.C. (1993). Focal attention produces spatially selective processing in visual cortical areas V1, V2, and V4 in the presence of competing stimuli. J. Neurophysiol. *70*, 909–919.

Motter, B.C. (1994). Neural correlates of feature selective memory and pop-out in extrastriate area V4. J. Neurosci. *14*, 2190–2199.

Moult, P.R. (2009). Neuronal glutamate and GABAA receptor function in health and disease. Biochem. Soc. Trans. *37*, 1317–1322.

Newsome, W.T., and Pare, E.B. (1988). A Selective Impairment of Motion Perception the Middle Temporal Visual Area (MT) Following Lesions of. J. Neurosci. *8*, 2201–2211.

Niell, C.M. (2011). Exploring the next frontier of mouse vision. Neuron *72*, 889–892.

Niell, C.M. (2014). Cell Types, Circuits, and Receptive Fields in the Mouse Visual Cortex. Annu. Rev. Neurosci. *38*, 150504162358003.

Niell, C.M., and Stryker, M.P. (2008). Highly Selective Receptive Fields in Mouse Visual Cortex. J. Neurosci. *28*, 7520–7536.

Niell, C.M., and Stryker, M.P. (2010). Modulation of visual responses by behavioral state in mouse visual cortex. Neuron *65*, 472–479.

Nienborg, H., Cohen, M.R., and Cumming, B.G. (2012). Decision-related activity in sensory neurons: correlations among neurons and with behavior. Annu. Rev. Neurosci. *35*, 463–483.

Nienborg, H., Hasenstaub, A., Nauhaus, I., Taniguchi, H., Huang, Z.J., and Callaway, E.M. (2013). Contrast dependence and differential contributions from somatostatin- and parvalbumin-expressing neurons to spatial integration in mouse V1. J. Neurosci. *33*, 11145–11154.

Noudoost, B., Chang, M.H., Steinmetz, N.A., and Moore, T. (2010). Top-down control of visual attention. Curr. Opin. Neurobiol. *20*, 183–190.

O'Connor, D.H., Fukui, M.M., Pinsk, M. a, and Kastner, S. (2002). Attention modulates responses in the human lateral geniculate nucleus. Nat. Neurosci. *5*, 1203–1209.

Ohki, K., and Reid, R.C. (2007). Specificity and randomness in the visual cortex. Curr. Opin. Neurobiol. *17*, 401–407.

Olivas, N.D., Quintanar-Zilinskas, V., Nenadic, Z., and Xu, X. (2012). Laminar circuit organization and response modulation in mouse visual cortex. Front. Neural Circuits *6*, 1–21.

Olsen, S.R., Bortone, D.S., Adesnik, H., and Scanziani, M. (2012). Gain control by layer six in cortical circuits of vision. Nature *483*, 47–52.

Pasupathy, A., and Connor, C.E. (1999). Responses to contour features in macaque area V4. J. Neurophysiol. *82*, 2490–2502.

Pfeffer, C.K., Xue, M., He, M., Huang, Z.J., and Scanziani, M. (2013). Inhibition of inhibition in visual cortex: the logic of connections between molecularly distinct interneurons. Nat. Neurosci. *16*, 1068–1076.

Pinto, L., Goard, M.J., Estandian, D., Xu, M., Kwan, A.C., Lee, S.-H., Harrison, T.C., Feng, G., and Dan, Y. (2013). Fast modulation of visual perception by basal forebrain cholinergic neurons. Nat. Neurosci. *16*, 1857–1863.

Piscopo, D.M., El-Danaf, R.N., Huberman, A.D., and Niell, C.M. (2013). Diverse Visual Features Encoded in Mouse Lateral Geniculate Nucleus. J. Neurosci. *33*, 4642–4656.

Platt, M.L., and Glimcher, P.W. (1999). Neural correlates of decision variables in parietal cortex. Nature *400*, 233–238.

Polack, P.-O., Friedman, J., and Golshani, P. (2013). Cellular mechanisms of brain state-dependent gain modulation in visual cortex. Nat. Neurosci. *16*, 1331–1339.

Poort, J., Khan, A.G., Pachitariu, M., Nemri, A., Orsolic, I., Krupic, J., Bauza, M., Sahani, M., Keller, G.B., Mrsic-Flogel, T.D., et al. (2015). Learning Enhances Sensory and Multiple Non-sensory Representations in Primary Visual Cortex. Neuron 1–13.

Pritchard, R.M. (1961). Stabilized Images on the Retina. Sci. Am. 72–79.

Prönneke, A., Scheuer, B., Wagener, R.J., Möck, M., Witte, M., and Staiger, J.F. (2015). Characterizing VIP neurons in the barrel cortex of VIPcre/tdTomato mice reveals layer-specific differences. Cereb. Cortex *25*, 4854–4868.

Prusky, G.T., and Douglas, R.M. (2004). Characterization of mouse cortical spatial vision. Vision Res. *44*, 3411–3418.

Prusky, G.T., West, P., and Douglas, R. (2000). Behavioral assessment of visual acuity in mice and rats. Vision Res. *40*, 2201–2209.

Purushothaman, G., Marion, R., Li, K., and Casagrande, V.A. (2012). Gating and control of primary visual cortex by pulvinar. Nat. Neurosci. *15*, 905–912.

Quiroga, R.Q., Nadasdy, Z., and Ben-Shaul, Y. (2004). Unsupervised Spike Detection and Sorting with Wavelets and Superparamagnetic Clustering. Neural Comput. *16*, 1661–1687.

Raposo, D., Kaufman, M.T., and Churchland, A.K. (2014). A category-free neural population supports evolving demands during decision-making. Nat. Neurosci. *17*, 1784–1792.

Remtulla, S. (1985). A schematic eye for the mouse, and comparisons with tha rat (vol.25, No.1, 1985 VISION RESEARCH).pdf. Vision Res. *25*, 21.

Rodgers, C.C., and DeWeese, M.R. (2014). Neural correlates of task switching in prefrontal cortex and primary auditory cortex in a novel stimulus selection task for rodents. Neuron *82*, 1157–1170.

Roelfsema, P.R., Lamme, V.A., and Spekreijse, H. (1998). Object-based attention in the primary visual cortex of the macaque monkey. Nature *395*, 376–381.

Roth, M.M., Helmchen, F., and Kampa, B.M. (2012). Distinct Functional Properties of Primary and Posteromedial Visual Area of Mouse Neocortex. J. Neurosci. *32*, 9716–9726.

Rudy, B., Fishell, G., Lee, S., and Hjerling-Leffler, J. (2011). Three groups of interneurons account for nearly 100% of neocortical GABAergic neurons. Dev. Neurobiol. *71*, 45–61.

Sachidhanandam, S., Sermet, B.S., and Petersen, C.C.H. (2016). Parvalbumin-Expressing GABAergic Neurons in Mouse Barrel Cortex Contribute to Gating a Goal-Directed Sensorimotor Transformation. Cell Rep. *15*, 700–706.

Sakatani, T., and Isa, T. (2007). Quantitative analysis of spontaneous saccade-like rapid eye movements in C57BL/6 mice. Neurosci. Res. *58*, 324–331.

Sanders, J.I., and Kepecs, A. (2012). Choice ball: a response interface for two-choice psychometric discrimination in head-fixed mice. J. Neurophysiol. *108*, 3416–3423.

Scholl, B., Tan, A.Y.Y., Corey, J., and Priebe, N.J. (2013). Emergence of Orientation Selectivity in the Mammalian Visual Pathway. J. Neurosci. *33*, 10616–10624.

Scholz, F.W., and Stephens, M.A. (1987). K-Sam ple Anderson-Da rl ing Tests. J. Am. Stat. Assoc. *82*, 37–41.

Schuett, S., Bonhoeffer, T., and Hübener, M. (2002). Mapping retinotopic structure in mouse visual cortex with optical imaging. J. Neurosci. *22*, 6549–6559.

Seabrook, T.A., Burbridge, T.J., Crair, M.C., and Huberman, A.D. (2017). Architecture, Function, and Assembly of the Mouse Visual System. Annu. Rev. Neurosci. *40*, 499–538.

Shenhav, A., Cohen, J.D., and Botvinick, M.M. (2016). Value, search, persistence and model updating in anterior cingulate cortex. Nat. Neurosci. *19*, 1280–1285.

Sherman, S.M., and Guillery, R.W. (1998). On the actions that one nerve cell can have on another: Distinguishing "drivers" from "modulators." Proc. Natl. Acad. Sci. *95*, 7121–7126.

Sherman, S.M., and Guillery, R.W. (2002). The role of the thalamus in the flow of information to the cortex. Philos. Trans. R. Soc. Lond. B. Biol. Sci. *357*, 1695–1708.

Shuler, M.G., and Bear, M.F. (2006). Reward Timing in the Primary Visual Cortex. Science (80-.). 1606–1610.

Sillito, A.M., and Jones, H.E. (2002). Corticothalamic interactions in the transfer of visual information. Philos. Trans. R. Soc. B Biol. Sci. *357*, 1739–1752.

Stahl, J.S., Van Alphen, A.M., and De Zeeuw, C.I. (2000). A comparison of video and magnetic search coil recordings of mouse eye movements. J. Neurosci. Methods *99*, 101–110.

Stanislaw, H., and Todorov, N. (1999). Attention_Calculation of signal detection theory measures. Behav. Res. Methods. Instrum. Comput. *31*, 137–149.

Stănişor, L., van der Togt, C., Pennartz, C.M. a, and Roelfsema, P.R. (2013). A unified selection signal for attention and reward in primary visual cortex. Proc. Natl. Acad. Sci. U. S. A. *110*, 9136–9141.

Tanaka, K. (1996). Inferotemporal cortex and object vision. Annu. Rev. Neurosci. *19*, 109–139.

Theeuwes, J., and Belopolsky, A. V. (2012). Reward grabs the eye: Oculomotor capture by rewarding stimuli. Vision Res. *74*, 80–85.

Treue, S., and Martínez Trujillo, J.C. (1999). Feature-based attention influences motion processing gain in macaque visual cortex. Nature *399*, 575–579.

Vaiceliunaite, A., Erisken, S., Franzen, F., Katzner, S., and Busse, L. (2013). Spatial integration in mouse primary visual cortex. J. Neurophysiol. *110*, 964–972.

Wallace, D.J., Greenberg, D.S., Sawinski, J., Rulla, S., Notaro, G., and Kerr, J.N.D. (2013). Rats maintain an overhead binocular field at the expense of constant fusion. Nature *498*, 65–69.

Wallis, J.D., and Kennerley, S.W. (2010). Heterogeneous reward signals in prefrontal cortex. Curr. Opin. Neurobiol. *20*, 191–198.

Wang, Q., and Burkhalter, A. (2007). Area map of mouse visual cortex. J Comp Neurol *502*, 275–290.

Wang, Q., Gao, E., and Burkhalter, A. (2011). Gateways of Ventral and Dorsal Streams in Mouse Visual Cortex. J. Neurosci. *31*, 1905–1918.

Wekselblatt, J.B., Flister, E.D., Piscopo, D.M., and Niell, C.M. (2016). Large-scale imaging of cortical dynamics during sensory perception and behavior. J. Neurophysiol. *115*, 2852–2866.

Willmore, B.D.B., Prenger, R.J., and Gallant, J.L. (2010). Neural Representation of Natural Images in Visual Area V2. J. Neurosci. *30*, 2102–2114.

Wilson, N.R., Runyan, C.A., Wang, F.L., and Sur, M. (2012). Division and subtraction by distinct cortical inhibitory networks in vivo. Nature *488*, 343–348.

Wimmer, R.D., Schmitt, L.I., Davidson, T.J., Nakajima, M., Deisseroth, K., and Halassa, M.M. (2015). Thalamic control of sensory selection in divided attention. Nature.

Wurtz, R.H. (1969). Response of striate cortex neurons to stimuli during rapid eye movements in the monkey. J. Neurophysiol. *32*, 975–986.

Zhang, F., Wang, L.P., Brauner, M., Liewald, J.F., Kay, K., Watzke, N., Wood, P.G., Bamberg, E., Nagel, G., Gottschalk, A., et al. (2007). Multimodal fast optical interrogation of neural circuitry. Nature *446*, 633–639.

Zhang, S., Xu, M., Kamigaki, T., Do, J.P.H., Chang, W.-C., Jenvay, S., Miyamichi, K., Luo, L., and Dan, Y. (2014). Long-range and local circuits for top-down modulation of visual cortical processing. Science (80-.). *54540*, 382–385.

Zhang, S., Xu, M., Chang, W.C., Ma, C., Hoang Do, J.P., Jeong, D., Lei, T., Fan, J.L., and Dan, Y. (2016). Organization of long-range inputs and outputs of frontal cortex for top-down control. Nat. Neurosci. *19*, 1733–1742.

Zhao, X., Chen, H., Liu, X., and Cang, J. (2013). Orientation-selective Responses in the Mouse Lateral Geniculate Nucleus. J. Neurosci. *33*, 12751–12763.

Znamenskiy, P., and Zador, A.M. (2013). Corticostriatal neurons in auditory cortex drive decisions during auditory discrimination. Nature *497*, 482–485.